

MSc Sustainable Energy Technology
Master Thesis

Dynamic Modelling and Techno-Economic Optimization of a Hydrogen Storage System as a Buffer Between Production and Supply Logistics

Author: Cas Lever, s3080218

Supervisor: dr. S. Hajimolana, dr. F. Khalighi, L.A. Jeronimo Oliveira

December, 2025

Department of Thermal and Fluid Engineering
Faculty of Engineering Technology,
Sustainable Energy Technology
University of Twente

UNIVERSITY OF TWENTE.

Abstract

The transition toward a sustainable energy system requires efficient hydrogen storage solutions that can balance the variability of renewable energy sources with a steady hydrogen supply. This thesis investigates the technical and economic performance of a compressed hydrogen buffer storage system designed for a hydrogen production plant in the Netherlands and evaluates potential design optimizations. The system connects hydrogen production from Proton Exchange Membrane (PEM) and Solid Oxide Electrolysis Cell (SOEC) electrolyzers to truck-based delivery through an underground hydrogen storage network.

A dynamic model was developed in Python to simulate the interaction between hydrogen production, storage compartments, and truck-based delivery via filling stations. Key parameters—including storage pressure configuration, logistical capacity, and operational days—were varied to assess their impact on system performance. Technical performance was evaluated using key performance indicators (KPIs) such as delivery delay, realized production, and hydrogen output. The best-performing configuration was then compared with the original design in terms of economic performance, using additional KPIs including energy costs and the Levelized Cost of Hydrogen Storage (LCHS).

Results show that increasing the number of filling stations and the number of operational days per week from five to six yields the most optimal performance, improving system stability and hydrogen output significantly. This required a higher storage capacity, achieved by adjusting the pressure configuration from 100–70 bar to 160–50 bar. Although the optimized design was slightly less energy efficient than the original, it was similar in terms of cost-efficiency due to lower average weekend electricity prices.

The optimized configuration reduced the LCHS from 0.91 €/kg to 0.72 €/kg and increased realized production by 52%. These results demonstrate that the optimized system significantly enhances both the technical and economic performance of the hydrogen buffer storage.

Contents

1	Introduction	2
1.1	Problem definition	3
1.2	Case Study Context	3
1.3	Research Question	3
1.4	Research Goal	4
1.5	Thesis structure	4
2	Theoretical Background	5
2.1	Hydrogen production	5
2.1.1	Proton Exchange Membrane (PEM) Electrolysis	5
2.1.2	Solid Oxide Electrolysis (SOE)	6
2.2	Hydrogen storage	7
2.2.1	Physical-based hydrogen storage	7
2.2.2	Material-based hydrogen storage	9
2.2.3	Compressors	9
2.2.4	Challenges and safety considerations with compressed storage	12
2.3	Hydrogen transportation	12
3	Methodology	14
3.1	System design	14
3.1.1	Hydrogen production	15
3.1.2	Storage system	15
3.1.3	Filling stations	16
3.2	Model Development	19
3.2.1	Model overview	19
3.2.2	Hydrogen production	19
3.2.3	Updating the state of the tanks	20
3.2.4	Filling tanks	24
3.2.5	Determining demand	24
3.2.6	Emptying tanks	26
3.3	Economic analysis (Levelized cost of hydrogen storage)	26
3.4	Simulation Scenarios: Technical Performance	28
3.4.1	Pressure	28
3.4.2	Logistical Capacity	28
3.4.3	Operational Days	29
3.5	Simulation Scenarios: Economic Performance	29
3.6	Key Performance Indicators: Technical Performance	29
3.7	Key Performance Indicators: Economic Performance	30

4 Results & Discussion	32
4.1 Model Verification	32
4.2 Scenario Testing: Technical Performance	37
4.2.1 Pressure Configuration	37
4.2.2 Logistical Capacity	39
4.2.3 Operational Days	42
4.2.4 Combination	45
4.2.5 Optimized scenario	46
4.3 Scenario Testing: Economic Performance	48
4.3.1 Energy Consumption and Costs	48
4.3.2 CAPEX	49
4.3.3 OPEX and LCHS	49
5 Conclusion	51
5.1 Recommendations	52
A Model Assumptions	56
B Thermodynamic calculations	58

List of Figures

2.1	PEM electrolysis process [1].	5
2.2	SOEC hydrogen production process [1].	6
2.3	Hydrogen storage methods overview [2].	7
2.4	Schematic representation of a reciprocating piston compressor. Extent of the piston's movement: Top Dead Centre (TDC) and Bottom Dead Centre (BDC). [3].	10
2.5	Schematic representation of a diaphragm compressor [3].	11
2.6	Schematic representation of a centrifugal compressor [3].	12
3.1	Overall System	15
3.2	Schematic overview of the filling stations.	16
3.3	Main overview of the model, with its main components.	19
3.4	Hydrogen production overview, with its inputs and to where the outputs are going.	20
3.5	Updating the tanks in emptying state	21
3.6	Updating tanks in Filling and Idle states. Determining whether tanks can transition to Emptying state.	22
3.7	Updating tanks in Filling state. Checking whether tanks are full and should transition to Idle state.	22
3.8	Updating tanks in Idle state. Determining whether tanks can transition to Filling state.	23
3.9	Process of filling tanks.	24
3.10	Process of determining hydrogen demand via the filling stations. The process for the active docking station is given in part A, and the process for the inactive docking station is given in part B.	25
3.11	Levelized cost of multiple hydrogen storage methods [4].	27
4.1	The outgoing hydrogen of a system during the second week under normal conditions and a configuration of 100-40. Simulation phases: start-up phase (yellow area), day shifts (green area), night shift (blue area), and non-operating days (red area).	33
4.2	The total net mass in the storage during one week using standard conditions and a pressure configuration of 100-40. Simulation phases: start-up phase (yellow area), day shifts (green area), night shift (blue area), and non-operating days (red area)	33
4.3	The hydrogen production for a simulation of one week.	35
4.4	Energy price data during a one week simulation.	35
4.5	Comparison of all pressure configurations, using standard conditions for the system (5 filling stations and 5 operational days).	37

4.6	The average delay per truck per pressure configuration, in a system with five, six, and seven filling stations.	39
4.7	The realized production (%) per pressure configuration, in a system with five, six, and seven filling stations.	40
4.8	The outgoing hydrogen per pressure configuration, in a system with five, six, and seven filling stations.	41
4.9	The average delay per truck per pressure configuration, in a system with five, six, and seven operational days per week.	42
4.10	The realized production per pressure configuration, in a system with five, six, and seven operational days per week.	43
4.11	The outgoing hydrogen per pressure configuration, in a system with five, six, and seven operational days per week.	44
4.12	Comparison of all pressure combinations for a system with six filling stations and six operational days.	45

List of Tables

2.1 Comparison of physical hydrogen storage methods.	8
4.1 Input values for the original and optimized system setups.	46
4.2 Technical output values for the original and optimized system designs. . . .	47
4.3 Energy performance comparison for the original and optimized system designs.	48
4.4 Capital investment cost comparison of system components.	49
4.5 Annual operational cost comparison for the original and optimized system designs.	49
4.6 Economic performance comparison between the original and optimized system designs.	50

Chapter 1

Introduction

The accelerating impacts of climate change have increased a global push towards clean and sustainable energy systems. Rising sea levels, increasing temperatures, and more frequent extreme weather events are among the major consequences of climate change [5]. In addition, geopolitical events such as the war in Ukraine have led to significant price fluctuations of fossil fuels and have highlighted the vulnerabilities of fossil fuel dependency [6].

The combination of the need to mitigate climate change and the desire to reduce reliance on importing fossil fuels has led to growing interest in sustainable energy in Europe. As a result, the European Union (EU) has set the long-term goal to be climate-neutral by 2050, requiring an economy with net-zero greenhouse gas emissions [7]. To achieve this goal, European countries must undergo the decarbonisation of their energy systems. The Netherlands, as one of the founding members of the EU, must also comply with these targets. The country wants to achieve this with its ambitious offshore wind targets. By the end of 2032, the Dutch government wants to have 21 gigawatts (GW) of offshore wind energy, and 70 GW by 2050 [8]. This will cover a significant part of the total electricity consumption of the Netherlands, but will also bring significant variability into its energy system.

A crucial part of the energy transition is the large-scale integration of renewable energy sources such as wind and solar power. However, these sources are dependent on weather conditions, which are not constant and reliable. The energy output of wind and solar is intermittent, which poses a challenge when requiring a steady energy supply. Additionally, while direct electrification is expected to play a central role in the energy transition, it is not a universal solution. Electricity can efficiently decarbonise many end-use sectors, such as residential heating and passenger transport, but several challenges remain. Some industrial processes and long-distance transport applications are difficult to electrify due to their high energy density requirements [9]. Hydrogen can address both problems: it can mitigate the intermittency of wind and solar power by serving as a versatile energy carrier and storage medium, and it can help decarbonise hard-to-abate sectors by enabling the production of ammonia, steel, and synthetic fuels for long-distance aviation and shipping [9]. The Dutch government has also realised the importance of hydrogen for the energy transition. The national hydrogen strategy of the Netherlands aims for 3 to 4 GW of electrolyser capacity by 2030 [10].

1.1 Problem definition

Hydrogen storage is widely recognised as a key enabler of the energy transition. While most discussions focus on large-scale or seasonal energy balancing, storage at the production-plant level also plays a crucial role by acting as a buffer between variable renewable hydrogen production and the steady requirements of supply logistics. The design of such storage is challenging: insufficient capacity risks delivery failures, whereas oversizing results in unnecessary costs. In addition to capacity, operational strategies must be managed carefully to minimise expenses and ensure feasibility. Compression, as one of the most energy-intensive steps in the hydrogen value chain, further complicates this challenge by making costs highly sensitive to fluctuating electricity prices. Despite its importance, the optimisation of buffer storage systems at the plant level remains mostly underexplored, creating uncertainty for companies aiming to integrate renewable hydrogen production with reliable and cost-efficient storage.

1.2 Case Study Context

This thesis is conducted in collaboration with ROGER Energy, a Dutch startup established in 2022 as a collaboration between a group of entrepreneurs and researchers from the University of Twente and Saxion University of Applied Sciences. The company specialises in the production, supply, and application of green hydrogen and is currently designing a hydrogen production plant in the Netherlands, powered by offshore wind energy. For such a facility, the feasibility and optimisation of the hydrogen buffer storage system is a key element of the overall plant design, ensuring reliable delivery and cost-effective operations. This improvement can help increase hydrogen usage in the Netherlands by enhancing the reliability and efficiency of hydrogen supply chains, thereby supporting the national transition toward a sustainable energy system.

1.3 Research Question

Based on the problem definition and the context of the case study, the following research question has been formulated:

What is the technical and economic performance of the proposed hydrogen buffer storage system, and how can its design be optimized to improve overall system performance?

This main research question is further divided into the following sub-questions:

1. How does the proposed hydrogen buffer storage system perform under realistic operating conditions?
2. How do changes in technical design parameters influence the performance of the hydrogen buffer storage system?
3. Which system configuration provides improved performance compared to the original design?
4. How do the original and optimized system configurations compare in terms of economic performance?

1.4 Research Goal

The main goal of this study is to assess the technical and economic performance of the proposed hydrogen buffer storage system that connects hydrogen production and truck-based delivery, and to propose and evaluate potential design optimizations. To achieve these goals, the following objectives are defined:

1. Simulate the proposed hydrogen storage system by building a model in Python and using data provided by ROGER Energy.
2. Test alternative system configurations by varying key parameters, and determine an optimized new scenario.
3. Analyse the technical and economic performance of the current and the new systems.

1.5 Thesis structure

The next chapter provides a theoretical background to give information about hydrogen production, storage, and transportation, with a focus on compressed hydrogen storage. Chapter 3 describes the designed system, explains the model developed in Python, and describes the simulation scenarios which will be performed. Chapter 4 presents and analyses the results of the simulations, assessing both technical and economic performance. Finally, Chapter 5 provides the conclusions of the study and gives recommendations.

Chapter 2

Theoretical Background

2.1 Hydrogen production

Hydrogen can be produced through various methods. The hydrogen produced in the production plant that is connected to the storage, will come from two different processes: Proton Exchange Membrane (PEM) and Solid Oxide Electrolysis cell (SOEC) electrolyzers. These production methods will be explained in the coming sections.

2.1.1 Proton Exchange Membrane (PEM) Electrolysis

With proton exchange membrane (PEM) electrolysis, water is split into hydrogen and oxygen via an electrochemical process. Water comes in contact with the anode and splits into oxygen, protons (H^+) and electrons (e^-). The protons then go through the membrane to the negatively charged cathode, while the electrons exit the anode through the external power circuit towards the cathode. At the cathode, the protons and electrons combine to form hydrogen gas [1]. This process is also displayed in Figure 2.1.

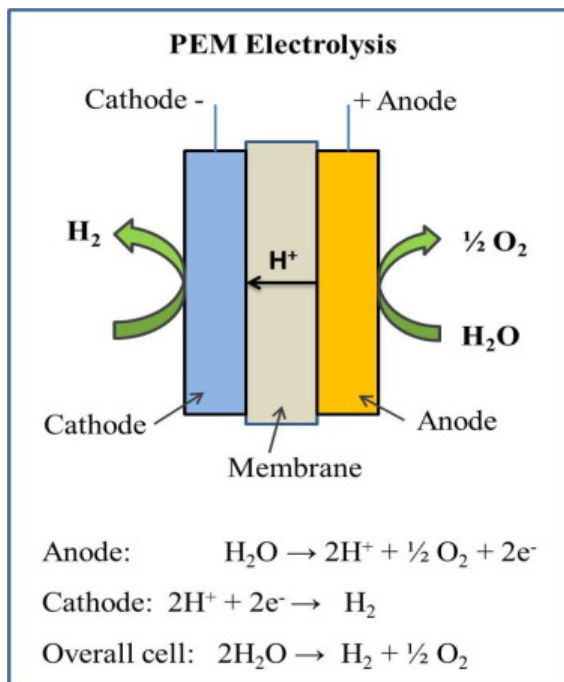


FIGURE 2.1: PEM electrolysis process [1].

PEM electrolyzers are attractive for industrial applications, as they are easy to balance due to their quick response time, allowing them to handle fluctuations in power input effectively [1]. Furthermore, PEM electrolyzers have other advantages, like low operating temperatures (20-80°C) and very pure hydrogen production [1] [11] [12]. A disadvantage of PEM electrolyzers are the costs of the components. The catalyst are made of noble metals such as *Pt/Pd* for the cathode and *IrO₂/RuO₂* for the anode [1].

2.1.2 Solid Oxide Electrolysis (SOE)

While in a PEM electrolyser, water is added to the anode, in a solid oxide electrolysis cell (SOEC) water is added to the cathode in the form of steam. By adding electricity, the steam is then separated into hydrogen gas and oxygen ions (O^{2-}). The oxygen ions move towards the positively charged anode and are then oxidized to oxygen gas. This process is schematically displayed in Figure 2.2 [1] [13].

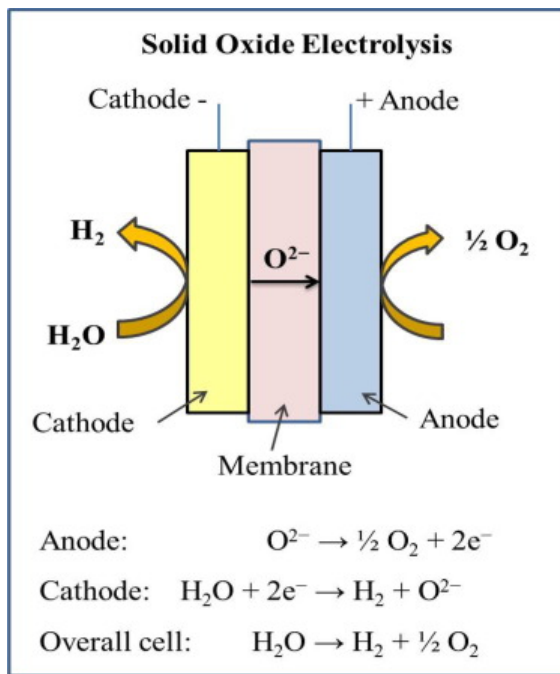


FIGURE 2.2: SOEC hydrogen production process [1].

This process happens at high temperatures (500-800°C), which allows it to incorporate waste heat from power plants or other industrial processes [12] [14]. The high operating temperature also allows for a reduced electrical energy demand, which is compensated for by the thermal energy [13]. This in turn increases energy efficiency, which reduces the costs.

While the PEM electrolyzer exhibits a fast dynamic response, the SOEC responds more slowly. This makes them a complementary combination, with the SOEC providing a stable baseline for continuous hydrogen production and the PEM compensating for short-term fluctuations in power supply or demand.

2.2 Hydrogen storage

Produced hydrogen needs to be stored first before it can be transported towards the consumer, as there often is a mismatch between production and demand. The main problem with hydrogen is that while it has a high energy density per unit mass (120 MJ/kg H_2), it has a low volumetric density (0.0824 kg/m^3). This results in a low volumetric energy density (0.01 MJ/L) at ambient conditions compared to conventional fuels like gasoline (32 MJ/L) [15]. Multiple hydrogen storage methods try to deal with this problem. These storage methods can be divided into two categories: physical based and material based storage (see Figure 2.3).

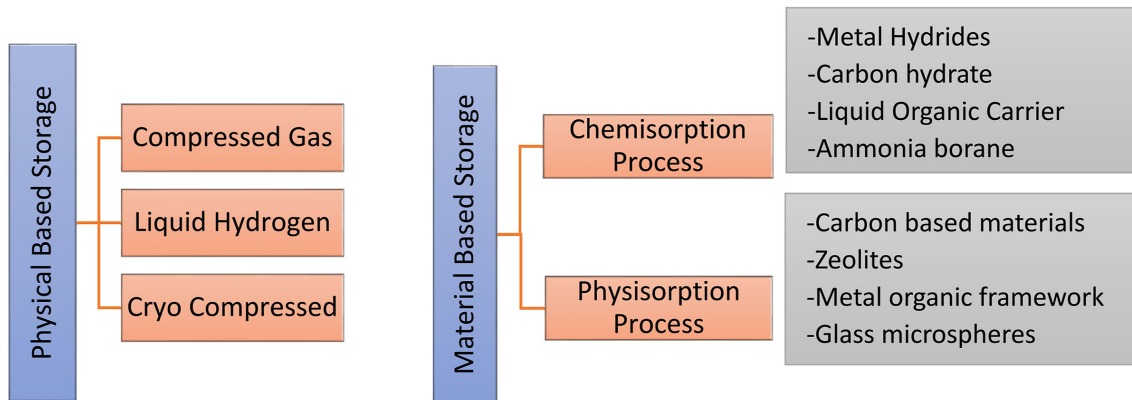


FIGURE 2.3: Hydrogen storage methods overview [2].

2.2.1 Physical-based hydrogen storage

Compressed hydrogen storage

The most used storage method is compressing hydrogen to high pressures. Here, hydrogen is compressed up to 700 bar to increase its volumetric energy density to 4.9 MJ/L [15]. However, this compression requires a large amount of energy and the tank's structural material needs to meet certain requirements. There are four types of compressed hydrogen storage tanks [15] [16] [17]:

- Type I: Made from metallic materials and capable of withstanding pressure up to 200-300 bar, but most commonly used up to 200 bar. It needs a thick metal layer, increasing the weight and reducing the net energy density. Common materials used are steel and aluminium alloys. This type is used mostly in industrial applications.
- Type II: The metallic wall is wrapped with fibre resin composite. This decreases the weight (30-40%), while increasing the costs (50%). It can withstand pressure up to 300 bar.
- Type III: Instead of metal, the tank body is made of carbon fibre composite materials lined with metals such as aluminium. They are strong and light but have low thermal conductivity, which may hinder heat release during compression. This type can allow pressures from 350-700 bar.
- Type IV: These are also made from carbon fibre composite materials, but instead of being lined with metal, it is lined with high-density polyethylene (HDPE). These tanks are light and can withstand pressure up to 700 bar.

Currently, type IV tanks are used the most for high-pressure storage due to their high capacity and lightweight design. However they are also the most expensive because of their high strength composites [18]. Also, disadvantages of compressed storage is that the hydrogen still occupies a significant volume (as its volumetric density of 4.9 MJ/L at 700 bar is still much lower than that of gasoline with 32 MJ/L). Furthermore the high pressure can increase the risks of leakage or ruptures, which poses a safety risk [18]. Despite these disadvantages, compressed hydrogen storage is a well-established and reliable method [2].

Liquid and Cryo-compressed storage

Besides compressing the hydrogen, it can also be stored in liquid form. Storing hydrogen as a liquid increases its volumetric density significantly (71 g/L at -253°C) and thus an increased volumetric energy density (8 MJ/L) [15]. Hydrogen needs to be cooled down to below -240°C (critical temperature of H_2) to be able to be liquefied and is liquefied at -253°C (boiling point of H_2 at 1 bar) [15]. Liquefied storage occurs at low pressures, allowing the storage tanks to be thin and inexpensive. Also, the liquid hydrogen density is 1.5-2 times higher than that obtained with compressed hydrogen, so the size of the storage tank is smaller. In liquid form, hydrogen is non-corrosive, so stainless steel and aluminium alloy tanks can be used for storage. However, the liquefaction process costs a lot of energy and money. Around 30-40% of the net heating value of hydrogen is used in this process.

There is also a combination of compressed hydrogen and liquid hydrogen, called cryo-compression. Hydrogen is stored at cryogenic temperatures (about -233°C). It is in a super-critical state (not liquid), because it is stored at 250-300 bar while the critical pressure of hydrogen is 13 bar [19]. It offers higher density than liquefied hydrogen (~80 g/L, nearly 10 g/L higher than liquefied hydrogen) [15] [19]. For this type of storage, a type III storage vessel is needed to cope with the high pressure, together with a thick insulation layer.

Physical-based methods comparison

The three types of physical-based hydrogen storage methods all have their advantages and disadvantages. Some relevant parameters, like volumetric density and volumetric energy density, are given in Table 2.1 [15] [20].

TABLE 2.1: Comparison of physical hydrogen storage methods.

Storage method	Volumetric H_2 density (g/L)	Volumetric energy density (MJ/L)	Operating Temp. (°C)	Operating pressure (bar)	Advantages	Disadvantages
Compressed gas	41.4	4.97	20	700	Mature technology and relatively simple design.	Safety concerns due to high operating pressure.
Liquid hydrogen	70.8	8.5	-253	1	High storage density and low-pressure operation.	High liquefaction energy demand and potential boil-off losses.
Cryo-compressed	80	9.6	-253	350	Combines high density with lower pressure requirements.	Complex and costly system with challenging thermal management.

Of the three methods, cryo-compressed has the highest volumetric density and volumetric energy density. However, it is very costly and comes with extra complexity. Liquid hydrogen is more used for intercontinental transport of hydrogen and aerospace applications,

as its biggest advantage is that it does not need to be pressurized. Finally, compressed hydrogen gas has the lowest density and energy density of the three, but is the most mature technology and is used the most in industrial applications and transport [2].

2.2.2 Material-based hydrogen storage

Material-based hydrogen storage systems store hydrogen within solid materials through either physisorption or chemisorption mechanisms. Another variant of material-based storage involves liquid organic hydrogen carriers (LOHCs), in which the storage medium is a liquid rather than a solid [15, 21]. One of the most promising LOHCs is methanol, which is formed from carbon dioxide and hydrogen. The advantage of methanol is that CO₂ can be obtained using direct air capture (DAC). However, retrieving hydrogen from methanol is a high-energy process (63.7 kJ/mol), and does emit greenhouse gases [22].

Currently, physisorption and chemisorption technologies are not suitable for large-scale industrial use, particularly in the context of this study. LOHC systems, however, show greater potential for industrial application because they can utilize existing gasoline storage and transportation infrastructure. Nevertheless, LOHCs produce a compound that contains hydrogen rather than pure hydrogen gas. To recover the hydrogen, the carrier must undergo a dehydrogenation reaction.

For these reasons, and because these methods do not meet the requirements of the system, material-based hydrogen storage methods will not be considered further in this study.

2.2.3 Compressors

Compressors are an important component of compressed hydrogen storage. Several types of compressors can be applied for hydrogen, with mechanical compressors being the most widely used in practice. These devices convert mechanical energy into internal energy by compressing the gas and increasing its pressure [3, 23]. Mechanical compressors are generally divided into two categories: positive displacement and dynamic compressors. Among these, positive displacement compressors are most commonly employed for hydrogen applications. They operate by confining a specific gas volume and subsequently reducing its size. This process increases the frequency of molecular collisions, thereby raising the pressure. A number of compressor designs are based on this principle, which will be discussed in the following subsections.

Reciprocating piston compressor

Reciprocating piston compressors are widely used in hydrogen applications, particularly when pressures above 30 bar are required. They are well suited for moderate flow rates combined with high-pressure operation [3, 23]. In practice, these compressors can achieve pressures up to 250 bar with flow rates as high as 890 kg/h. To maintain the high gas purity required for hydrogen, oil-free variants are employed. Furthermore, to mitigate the effects of hydrogen embrittlement, the cylinders can be equipped with protective liner coatings. The compressor consists of a piston–cylinder system with two automatic valves, driven by a crank mechanism that converts rotary motion into linear motion. The reciprocating movement of the piston compresses the hydrogen by reducing the gas volume and thereby increasing the pressure. A schematic representation of this process is shown in Figure 2.4.

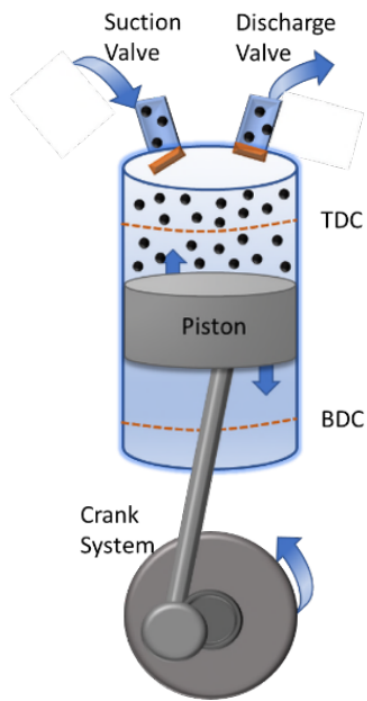


FIGURE 2.4: Schematic representation of a reciprocating piston compressor. Extent of the piston's movement: Top Dead Centre (TDC) and Bottom Dead Centre (BDC). [3].

Diaphragm compressor

The diaphragm compressor is based on the same operating principle as the reciprocating piston compressor, but with additional components inserted between the piston and the gas. The motion of the piston is transferred to a hydraulic fluid, which subsequently acts on a thin metal membrane known as the diaphragm [3, 23]. This arrangement ensures that the hydrogen remains completely isolated from the hydraulic system. This configuration makes the diaphragm compressor particularly suitable for high-purity gases, since the hydrogen does not come into direct contact with the piston. An additional advantage of this design is its relatively high efficiency, as the hydraulic fluid can be effectively cooled. However, diaphragm compressors suffer from limited durability, which restricts their use to applications with relatively low flow rates. A schematic representation of the diaphragm compressor is shown in Figure 2.5.

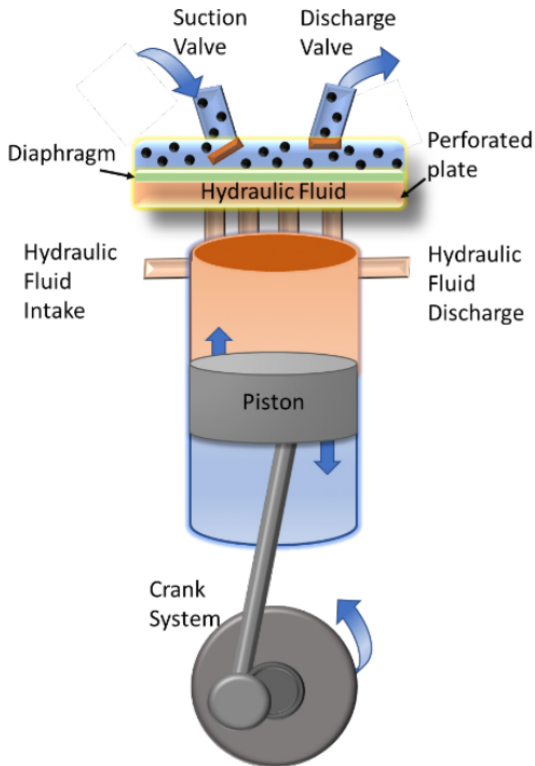


FIGURE 2.5: Schematic representation of a diaphragm compressor [3].

Centrifugal compressor

The centrifugal compressor is a representative example of a dynamic compressor and is primarily employed in applications requiring high flow rates and moderate compression ratios. Its working principle is based on the conversion of kinetic energy into pressure, achieved by accelerating the gas through an impeller and subsequently decelerating it in a diffuser. A schematic of the centrifugal compressor is shown in Figure 2.6.

Centrifugal compressors are widely used for air and natural gas compression in petrochemical plants and transmission pipelines. The achievable compression ratio depends strongly on the molecular weight of the gas. For hydrogen, which has a very low molecular weight, impeller tip speeds must be approximately three times higher than those used for natural gas. This requirement poses significant engineering challenges due to material strength limitations and the risk of hydrogen embrittlement [3].

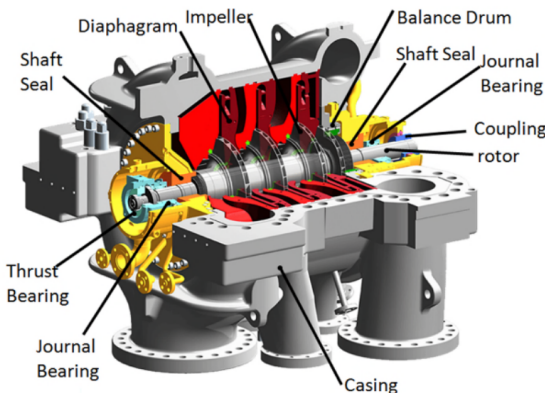


FIGURE 2.6: Schematic representation of a centrifugal compressor [3].

2.2.4 Challenges and safety considerations with compressed storage

Compressed hydrogen storage does have its disadvantages. It does have a low volumetric density (4.9 MJ/L at 700 bar [15]). It also requires 5 to 15% of its stored energy for its compression [24]. Furthermore, a general problem for hydrogen storage in metallic containers is hydrogen embrittlement. Hydrogen embrittlement affects metallic materials that come in contact with hydrogen (particularly steel). This effect results in the degradation of the metal's mechanical properties and premature cracking. This is caused by the dissolution of hydrogen atoms into the metal [25].

A big challenge that compressed hydrogen storage (and the use of hydrogen in general) faces is safety. Hydrogen faces safety challenges due to its high flammability and its ability to escape containment because of its small molecular size. These are especially problems with physical-based storage methods, as hydrogen is kept in its molecular form and is under extreme conditions. This requires robust safety measures, including sensitive leak detection systems, pressure relief valves and minimization of possible accidents [2].

2.3 Hydrogen transportation

The last step in the hydrogen supply chain is transportation. Here, hydrogen is taken from the storage and delivered to the customer. This study will limit itself to gaseous hydrogen storage. In gaseous form, hydrogen is compressed and stored in one of the four types of pressure tanks (see Section 2.2.1). This method is widely used due to its relatively low cost and well-established infrastructure [26]. The compressed hydrogen is most commonly transported with high-pressure tube trailers and pipelines. Tube trailers are mostly transported to end-users via road, but can also be transported via rail or ship. The tube trailers have a pressure range of 200-500 bar, either in a big cylinder tank or 20-40 smaller tubes [27]. At the destination, the compressed hydrogen is connected directly to end-user applications. Pipelines can also be used to transport hydrogen over long distances. However, the pipeline must be compatible with hydrogen to avoid issues like hydrogen embrittlement (see Section 2.2.4) [26]. This effect can be mitigated by using a material with high resistance to this effect. Some of these materials are austenitic stainless steels, nickel-based alloys and certain aluminium alloys [26]. Also using non-metallic materials, like composites or polymers, can eliminate the risk of embrittlement [26]. Nonetheless, using

pipelines for hydrogen transportation requires significant investment in the construction of infrastructure and its maintenance.

Chapter 3

Methodology

The purpose of this chapter is to describe the methodological approach used to investigate the research goal defined in Chapter 1. Specifically, the study aims to evaluate the technical and economic performance of the hydrogen buffer storage system proposed by ROGER Energy, and develop potential design optimizations. To achieve this goal, a dynamic simulation model of the plant's hydrogen storage system was developed in Python. The model reflects the company's proposed design but incorporates necessary assumptions and simplifications to enable scenario testing and comparative analysis. The methodology is structured in four parts. First, the overall system design is described, including production, storage, compression, and filling logistics. Second, the modelling approach is outlined, with an emphasis on the representation of hydrogen flows and operational constraints. Third, the simulation scenarios are presented, in which key parameters are systematically varied to test alternative configurations. Finally, the key performance indicators (KPIs) are defined, which serve as the basis for evaluating the technical and economic performance of the system across all scenarios. For the system design and the development of the model, multiple assumptions had to be made. These assumptions will be explained in the text, but an overview of the assumptions is given in Appendix A.

3.1 System design

The hydrogen storage system integrates renewable power generation, hydrogen production, underground storage, and final delivery to customers. An overview of the entire system is shown in Figure 3.1. Electricity from offshore wind turbines is converted into hydrogen using Proton Exchange Membrane (PEM) and Solid Oxide Electrolysis Cell (SOEC) electrolyzers. The produced hydrogen enters an underground storage system consisting of multiple compartments, which serve as a buffer capacity between variable production and demand. Hydrogen can be withdrawn through a limited number of outlets, each connected to compressors that can raise the pressure to 200 bar. The flows are then combined and further compressed to 500 bar for distribution via filling stations, where containers are loaded for transport to customers. In the following subsections, the individual components of the system are described in more detail.

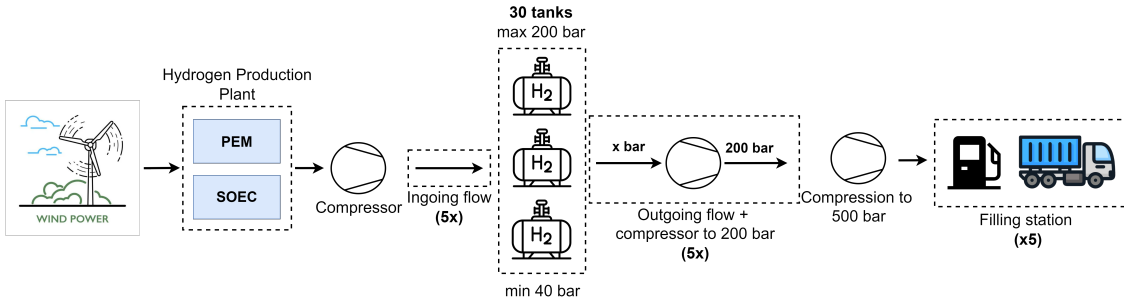


FIGURE 3.1: Overall System

3.1.1 Hydrogen production

The hydrogen entering the storage originates from the production plant, which consists of Proton Exchange Membrane (PEM) and Solid Oxide Electrolysis Cell (SOEC) electrolyzers. The total installed power capacity of the production plant is 19.4 MW. Since the plant has not yet been constructed, assumptions regarding the production flow are required.

The production plant will be connected to offshore wind turbines, and it is therefore assumed that the electricity supply is entirely sourced from wind power. To obtain realistic production data, wind speed measurements from 2015 are used, recorded at 10-minute intervals over a full year. The assumed reference turbine is the Multibrid M5000, an offshore turbine with a rated power of 5 MW and a hub height of 90 m [28]. To reach the target capacity of 19.4 MW, at least four turbines are required. However, due to variations in wind conditions, the nominal 19.4 MW is not always achieved. ROGER assumes 5,519 full load hours per year, which is 63% of the year. By applying the turbine's power curve to the wind data and aiming for an average capacity factor of approximately 63%, the number of turbines included in the model is set to 12, which achieves a capacity factor of 62.36%. All the power that is generated above 19.4 MW will be sent to the grid.

3.1.2 Storage system

After hydrogen is produced, it must be stored to balance the mismatch between variable production and relatively steady or scheduled demand. The company has proposed an underground piping-based storage system, which is divided into 30 compartments. Each compartment functions as an individual hydrogen storage tank with its own pressure conditions. While the compartments operate independently, they are constrained between a minimum and maximum pressure. The lower limit ensures that the system always remains pressurized, whereas the upper limit prevents the tanks from exceeding safety levels, which considers the tank's physical integrity.

The storage is designed as a metallic system, which classifies it as Type I compressed hydrogen storage. Based on this classification, the maximum operating pressure is set to 200 bar (see Chapter 2.2.1).

The overall storage capacity depends on the volume and pressure of the compartments. For the company's proposed system, the total storage volume is 3221 m³. Within the allowed pressure range, this defines the total hydrogen capacity of the buffer.

In addition to the physical layout, the storage system follows an operational control logic that governs the filling and withdrawal of hydrogen across the compartments. This logic ensures that hydrogen flows are balanced, pressures remain within safe limits, and storage is used efficiently under varying production and demand conditions. The design and implementation of this operational control logic are described in more detail in Chapter 3.2.

3.1.3 Filling stations

The final step in the system is the transfer of hydrogen from storage to customers. The hydrogen that is sold is transported in containers via truck transport, which operate at 500 bar. Since the storage operates at lower pressures, the withdrawn hydrogen must be compressed to 500 bar before it can be delivered.

This process is facilitated by filling stations, which connect the storage system to the containers. Each filling station consists of two docking positions, each capable of holding one truck with a container. During operation, one docking position is active while the other remains inactive. Once the active container has been filled, the station switches to the other dock, allowing the next container to be filled. This alternating setup aims to provide a continuous filling process, which would reduce stress on the system's components.

The company's design includes a total of five filling stations, allowing up to five containers to be filled simultaneously. A schematic overview of the filling system is shown in Figure 3.2.

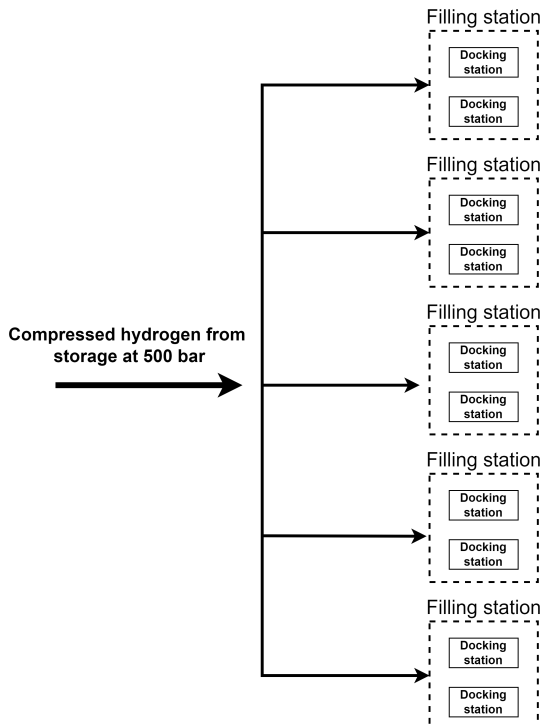


FIGURE 3.2: Schematic overview of the filling stations.

In practice, the containers used vary in size. However, for the sake of consistency in this research, a single representative container type is assumed. This container has a capacity of 280 kg of hydrogen at 500 bar. This simplification allows the outflow process to be modelled more consistently while still capturing the key operational characteristics.

Operational constraints

In addition to the technical design of the filling stations, several operational constraints apply to the proposed system:

- **Maximum flow rate:** Each filling station has a maximum hydrogen flow rate of 90 kg/h. This directly determines the filling time of a container and therefore limits the overall throughput capacity of the system.
- **Weekend operations:** No hydrogen off-take occurs during weekends. While hydrogen production continues, no containers are filled or transported during this period, which may lead to higher storage levels.
- **Shift schedule:** The facility operates under three shifts: 07:00–15:00, 15:00–23:00, and 23:00–07:00. Although hydrogen production runs continuously, the filling stations are only staffed during the two daytime shifts. During the night shift (23:00–07:00), no new trucks can arrive at the facility.
- **Night-time compressor operation:** Due to noise regulations, compressors cannot run at full capacity during the night shift. Containers that begin filling shortly before the night shift remain connected throughout the night, but filling proceeds at a reduced flow rate. It is assumed that the flow rate is such that trucks can fill overnight, leading to a flow rate of 35 kg/h.

These constraints significantly influence the interaction between hydrogen production, storage, and outflow. They introduce temporal variability in the system's ability to deliver hydrogen, which is explicitly considered in the modelling and analysis presented in Chapter 3.2.

Compressor Selection

Selecting an appropriate compressor type requires consideration of the specific operational requirements of the system. In this case, the compressor must be capable of handling medium to high flow rates of up to 450 kg/h, while ensuring compatibility with high-purity gases and with hydrogen in particular. Based on these requirements, the reciprocating piston compressor is identified as the most suitable option (see Chapter 2.2.3). Its proven ability to combine relatively high pressures and flow rates with adaptability for hydrogen applications makes it the best fit for the system under study.

Compressor stage and energy calculations

In the system, hydrogen operates at high pressures (up to 500 bar). At these high pressures, the thermodynamic behaviour of hydrogen deviates significantly from the ideal gas law. To account for this, the thermophysical property library *CoolProp* is used [29]. *CoolProp* enables accurate calculation of thermodynamic properties such as enthalpy and entropy under specified pressure and temperature conditions.

The hydrogen produced enters the compression system at 40 bar and 10°C. To enable storage, its pressure must be increased to the maximum allowable storage pressure. During compression, the temperature of the hydrogen rises rapidly. If compressed in a single stage, the temperature increase would exceed safe limits; therefore, intercooling is applied. The overall compression is divided into multiple stages, with the hydrogen cooled back to its initial temperature of 10°C between stages. The maximum allowable hydrogen temperature during compression is limited to 85°C, in accordance with safety guidelines for hydrogen refuelling [30].

The number of compression stages is determined based on this temperature limit. For an assumed number of stages N , the pressure ratio is equally divided across all stages. CoolProp is then used to evaluate the resulting outlet temperature of each stage. The smallest number of stages for which the outlet temperature remains below 85°C is selected. Following this approach, compression to 100 bar requires two stages, while compression to 120 bar and above requires three stages. Discharging the storage is done with two separate compressor systems. First, the hydrogen is compressed to 200 bar. This step requires a two-stage compressor when the minimum pressure is 70 bar, and a three-stage compressor when the minimum pressure is lower. The second step for discharging is to compress the hydrogen from 200 bar to 500 bar. This step requires two compressor stages.

To determine the energy required for compression, the thermodynamic properties of hydrogen were calculated using CoolProp. For each stage, the inlet enthalpy and entropy were determined at the current pressure and temperature. From this, the isentropic enthalpy was determined, and the real enthalpy is then determined by using the isentropic efficiency, which is taken as 65% based on literature values [3]. The difference between the inlet and outlet enthalpy represents the compressor work for that stage.

Between the stages, the hydrogen is cooled back to 10°C at the stage outlet pressure. The difference in enthalpy between the hot outlet state and the cooled state corresponds to the amount of heat that must be removed. This heat removal is performed by electrically driven chillers with an assumed coefficient of performance (COP) of 3, based on literature [31]. Using heat exchangers to recover this heat was also considered. However, because the compressor outlet temperature is limited to 85 °C, the available heat stream is relatively low-grade and cannot reach temperatures high enough to be useful elsewhere in the system. Additionally, fluctuations in production and storage operations introduce variability in the heat generation rate, making the heat stream irregular and unsuitable for stable heat recovery.

The total specific energy consumption is the sum of the compressor work of all stages, corrected by the mechanical efficiency of the compressor (assumed to be 90%), and the electrical energy required for cooling. This specific energy consumption (per kilogram of hydrogen) is then multiplied by the hydrogen mass flow rate to obtain the total energy consumption per simulation time step.

More detailed calculations with the actual formulas are given in Appendix B.

3.2 Model Development

This section will describe and explain the model that was made to simulate the hydrogen storage. The model took into account realism while also making certain assumptions to be able to compare different scenarios. Furthermore, the model has been made as flexible as possible to be able to change different variables easily. To explain the model, first, a total overview of the model will be given. After that, the explanation will go into more detailed parts of the model. An overview of the assumptions made for the model can be found in Appendix A.

3.2.1 Model overview

The model simulates a hydrogen storage with ingoing hydrogen from production, and outgoing hydrogen from demand. The model was made in Python, using the Numpy, Pandas, and Matplotlib libraries. The model simulates dynamically and does so per minute. The model also uses the CoolProp library (for thermodynamic properties). The overview of the model with its main components is given in Figure 3.3.

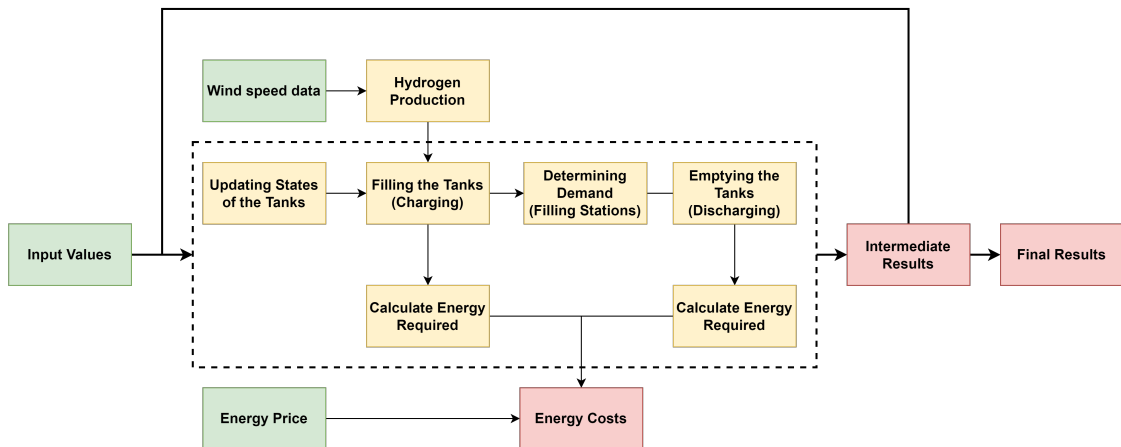


FIGURE 3.3: Main overview of the model, with its main components.

In Figure 3.3 and the subsequent figures illustrating the model, a consistent colour scheme is applied to identify different system functionalities. Green indicates system inputs, yellow represents processes, and red signifies system outputs.

The main inputs for the model are the system specifications, like the minimum and maximum pressure, and the length of the simulation. Other inputs are the wind speed data and the energy price, which are both time-dependent. The main process (within the dotted lines) repeats itself every iteration until the required number of iterations is reached. Intermediate results are saved and used again for the next iteration, while cumulative values are being saved. After the last iteration, the final result is given.

3.2.2 Hydrogen production

The hydrogen that comes into the storage is the hydrogen that is produced in the hydrogen production plant. The hydrogen production is based on electricity generated by offshore wind turbines. As mentioned in Chapter 3.1.1, the wind turbine used for this simulation is the Multibrid M5000 with a rated power of 5 MW. The total power capacity of the

production plant is 19.4 MW, with a goal of achieving a capacity factor of approximately 63%. To achieve this, the number of wind turbines that are required is 12.

The total power capacity of the production plant is divided between the two production methods: PEM and SOEC. The production comes largely from the SOEC, which has a capacity of 14.4 MW. The PEM electrolyzers have a capacity of 5 MW. As the PEM is more able to deal with fluctuations than the SOEC, the division of power is as follows: The SOEC runs with all generated power, up until 14.4 MW. If more power is generated, this will go towards the PEM. If more than 19.4 MW is generated, then this will go towards the grid.

To get the total power production, 10-minute average wind speeds are taken from the wind data from 2015. These are then used, with the type and number of wind turbines, to determine the generated power. The hydrogen production is then calculated using power curves for the PEM and SOEC. A schematic overview of this process is given in Figure 3.4.

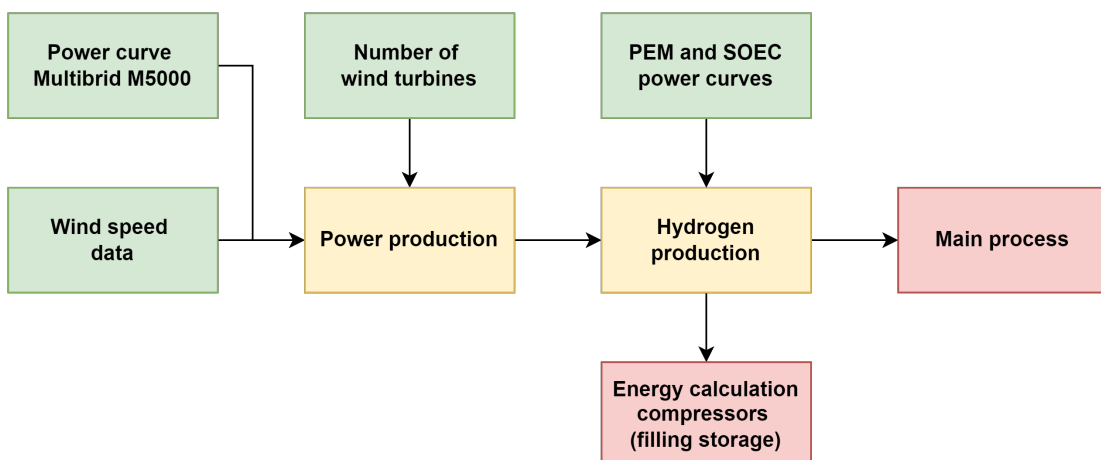


FIGURE 3.4: Hydrogen production overview, with its inputs and to where the outputs are going.

3.2.3 Updating the state of the tanks

The operation of the storage system involves not only the filling and emptying of tanks, but also the continuous updating of each tank's state. At any point in time, a tank can be in one of three states: **Filling**, **Emptying**, or **Idle**.

- In the *Filling* state, the tank is actively being charged with hydrogen.
- In the *Emptying* state, the tank is discharging hydrogen to meet demand.
- In the *Idle* state, no mass transfer occurs.

There is only a limited number of tanks that can be in the *Filling* or *Emptying* state at any given time. A maximum of five tanks can be in the *Filling* state and another five in the *Emptying* state. The remaining tanks must therefore be in the *Idle* state.

Updating tanks in Emptying state

Once the process is running and tanks are being emptied, each iteration a control is performed to check if the tanks that are currently in *Emptying* state can remain there. The decision process for this is schematically illustrated in Figure 3.5.

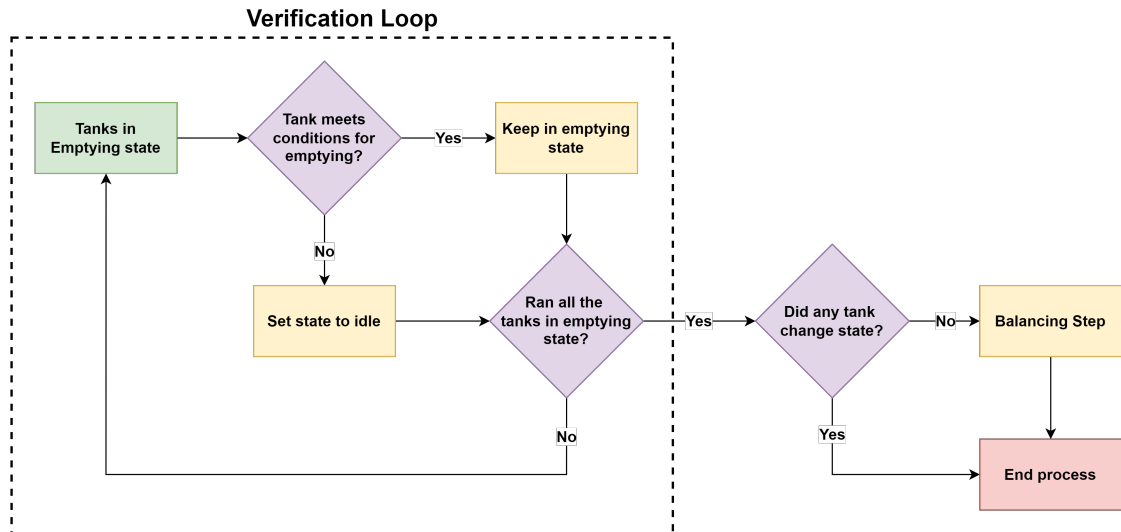


FIGURE 3.5: Updating the tanks in emptying state

As shown in Figure 3.5, certain conditions must be met for a tank to remain in *Emptying* state. The requirements for these tanks are:

1. The tank pressure must remain above the specified minimum pressure.
2. If there is no hydrogen demand in the system, the mass of hydrogen in the tank must be greater than the amount required to fill a single container. This prevents the system from entering a deadlock where tanks contain too little hydrogen to fill a container but too much to leave the *Emptying* state.
3. It must not be a period during which hydrogen withdrawal is disallowed (e.g. week-ends). During the non-operational period, all tanks should either be in *Filling* or *Idle* state, as they can then fill up during this period.

If a tank in the *Emptying* state no longer satisfies any of these requirements, it transitions to the *Idle* state. After all tanks in the *Emptying* state have been checked, the system evaluates whether any state changes have occurred. If no transitions take place and all *Emptying* tanks remain unchanged, a balancing step is performed. In this step, the tank with the lowest mass in the *Emptying* state is switched with the tank holding the largest mass among those in the *Filling* or *Idle* state. This reassignment ensures that not all *Filling* tanks become fully charged, which would otherwise result in wasted hydrogen. The switch is only executed if the relative difference in mass between the two tanks exceeds 10%.

Updating tanks in Filling and Idle state

After the tanks in the *Emptying* state have been updated, the system proceeds to update the tanks in the *Filling* and *Idle* states. The process consists of three steps: assigning new *Emptying* tanks, updating *Filling* tanks, and updating *Idle* tanks.

The process of assigning new tanks to *Emptying* state is displayed in Figure 3.6.

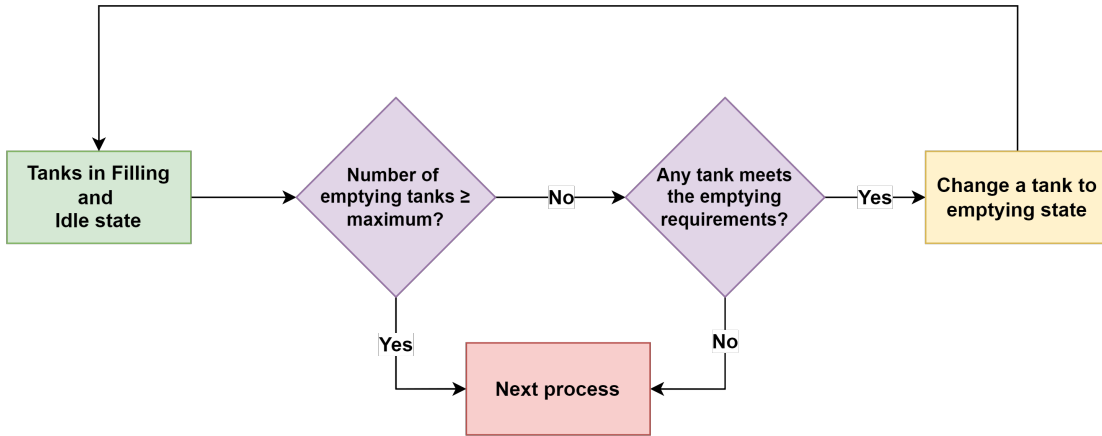


FIGURE 3.6: Updating tanks in Filling and Idle states. Determining whether tanks can transition to Emptying state.

First, the system checks whether there is capacity for additional tanks to enter the *Emptying* state, as the maximum for this is five. If capacity is available, all tanks in the *Filling* and *Idle* states are evaluated to determine whether they contain sufficient hydrogen to transition into *Emptying*. Whenever a tank meets this requirement, it is reassigned to the *Emptying* state. This process is repeated until either the maximum number of tanks in *Emptying* is reached, or no further tanks satisfy the condition. After this process, the system checks the tanks currently in the *Filling* state (shown in Figure 3.7).

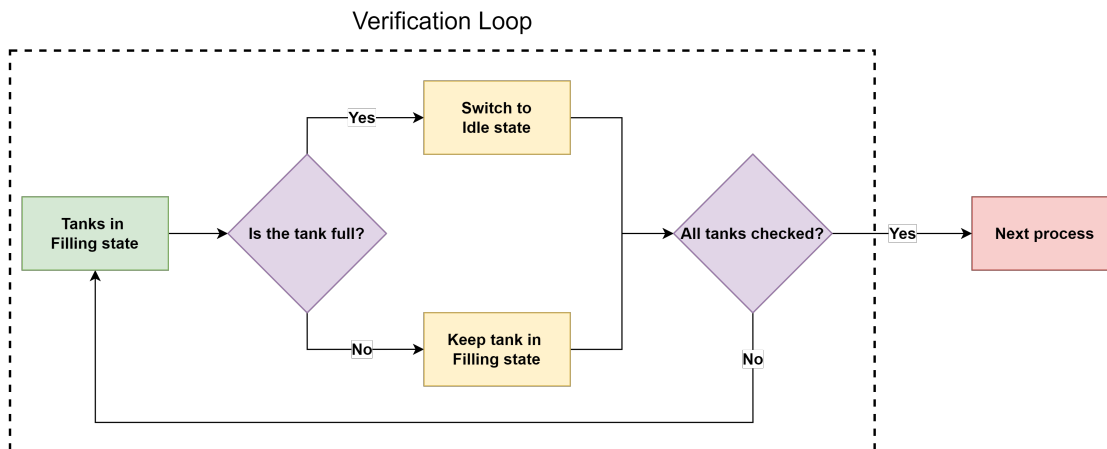


FIGURE 3.7: Updating tanks in Filling state. Checking whether tanks are full and should transition to Idle state.

If a tank becomes full, it is switched to the *Idle* state. This prevents overfilling and ensures that filling slots remain available for empty tanks. Finally, tanks in the *Idle* state are evaluated to determine whether they can transition to *Filling* (displayed in Figure 3.8).

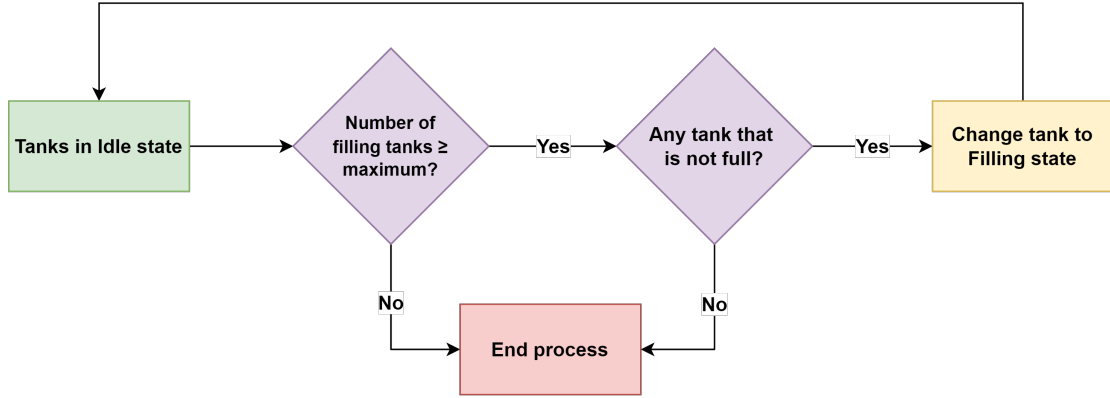


FIGURE 3.8: Updating tanks in Idle state. Determining whether tanks can transition to *Filling* state.

For tanks to switch from *Idle* to *Filling* state, the following two conditions must be met:

1. The total number of tanks in the *Filling* state must remain below the maximum allowed (five).
2. The tank must not be full (not be at maximum pressure).

If both conditions hold, the tank transitions from *Idle* to *Filling*.

3.2.4 Filling tanks

After the state of each tank has been updated, the actual processes are executed. The first process is the filling of tanks (see Figure 3.9). The hydrogen produced is directed towards all tanks in the *Filling* state.

In principle, the hydrogen is distributed equally among these tanks. However, if one tank is close to reaching its maximum capacity, it is filled to capacity first, and the remaining hydrogen is then divided among the other tanks. If the hydrogen production rate exceeds the total available capacity of the filling tanks, the surplus hydrogen is removed from the system and recorded as unhandled hydrogen.

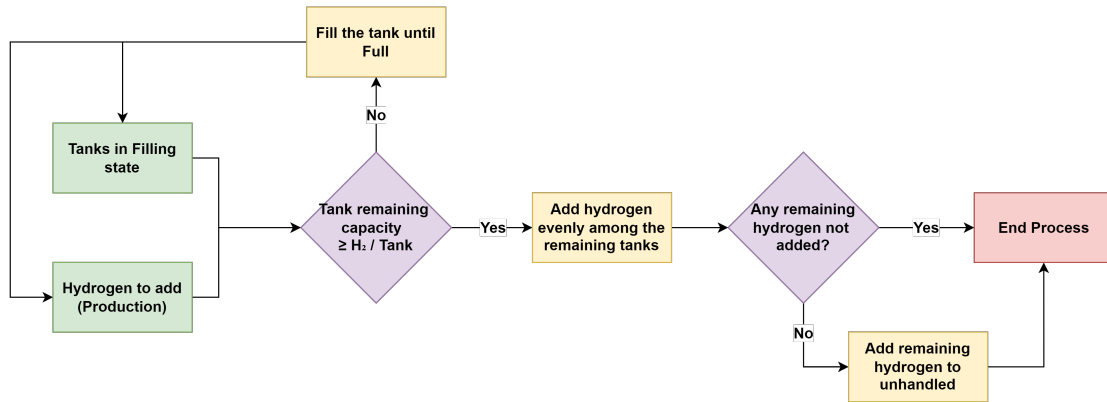


FIGURE 3.9: Process of filling tanks.

3.2.5 Determining demand

After the filling process has been completed, the next step is to determine the hydrogen demand and the amount that must be withdrawn from the tanks in the *Emptying* state. Demand occurs via the filling stations, each of which consists of two docking stations. At any time, one dock is active and connected to a truck, while the other dock is inactive and must wait until the active dock has finished. The processes for the active and inactive docking stations are given in Figure 3.10.

Prior to executing the process, the system determines whether the current time corresponds to a non-operational period. If so, hydrogen withdrawal is not permitted, and demand is set to zero. Otherwise, the system continues with the process of the active and inactive docking stations.

The first step for the active dock is to verify whether it has already reserved hydrogen. If no reservation exists, the system evaluates three conditions:

1. Whether there is sufficient time to complete a truck filling before the night shift begins.
2. Whether the night shift is already active.
3. Whether sufficient hydrogen is available to allocate a full truck filling.

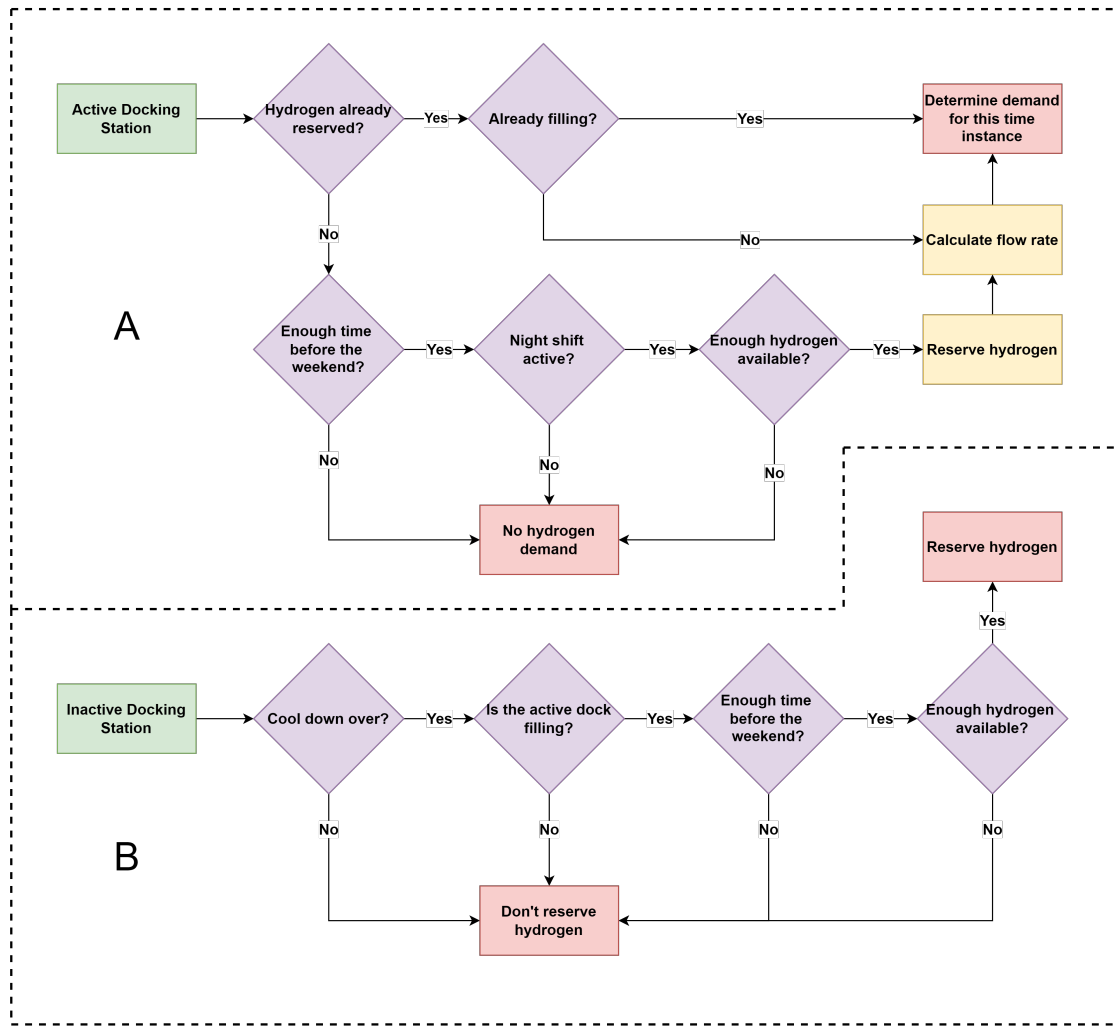


FIGURE 3.10: Process of determining hydrogen demand via the filling stations. The process for the active docking station is given in part A, and the process for the inactive docking station is given in part B.

If there is not enough time before the night shift or the night shift has already started, no hydrogen is reserved, and the dock misses its filling opportunity. If sufficient time and hydrogen are available, the full truck demand is reserved for that docking station.

Once a docking station has successfully reserved hydrogen, the required flow rate for filling is determined. Under normal conditions, this flow rate is set to the maximum value of 90 kg/h. However, operational constraints may occur during the night shift and non-operational periods. As discussed in Chapter 3.1.3, the flow rate must be reduced at night due to noise regulations. It is therefore assumed that a truck can be filled over the course of the 8-hour night shift, corresponding to a reduced flow rate of 35 kg/h.

To ensure that each truck can be filled during the night shift, the preceding truck's filling process must be synchronized accordingly. This means it must finish within a specific time window before the start of the night shift, which may require a slight adjustment of its flow rate based on the timing conditions.

The real-world ROGER system will operate using a reservation mechanism. In the model, each reservation slot is assumed to correspond to the time required to fill a truck at the maximum flow rate—3.11 hours for a 280 kg container at 90 kg/h. Thus, the model represents continuous operation, with all reservation slots fully utilized throughout the simulation period. The turnaround time, defined as the interval before the next truck arrives, is therefore set equal to this 3.11 hours, corresponding to the minimum filling time.

After the flow rate has been calculated, the active dock begins filling the truck. The flow rate remains constant until the truck is fully loaded. Meanwhile, if the inactive dock has completed its turnaround time (i.e. a new truck has arrived), it may already attempt to reserve hydrogen. If successful, it can proceed directly to the flow-rate calculation once it becomes active.

3.2.6 Emptying tanks

Once the hydrogen demand at each filling station has been determined, the withdrawal process from the tanks in the *Emptying* state can proceed. This process specifies how the required hydrogen is distributed among the available tanks.

First, all tanks in the *Emptying* state are sorted in ascending order of their mass content. Starting from the least-filled tank, the system checks whether the tank can supply the average hydrogen demand, defined as:

$$\dot{m}_{\text{avg}} = \frac{\dot{m}_{\text{demand}}}{n_{\text{emptying}}} \quad (3.1)$$

where \dot{m}_{demand} is the total hydrogen demand and n_{emptying} is the number of tanks currently in the *Emptying* state.

If the tank cannot supply \dot{m}_{avg} , it discharges its remaining hydrogen until it is empty. The total demand and number of active emptying tanks are then updated, and a new average demand is calculated. The procedure is repeated iteratively for the next tank in the sorted list.

This method ensures that nearly empty tanks are fully discharged first, while the remaining demand is automatically redistributed among the fuller tanks. In this way, the system both maximizes tank utilization and guarantees that overall hydrogen demand is met.

3.3 Economic analysis (Levelized cost of hydrogen storage)

If hydrogen storage is going to be a widely used energy storage method, it needs to be financially viable. The cost to store hydrogen can be expressed in the levelized cost of hydrogen storage (LCHS). LCHS can be described as the net present cost of the storage system divided by its cumulative hydrogen storage over the plant's entire lifetime [4]. The formula to calculate the LCHS is given in Equation 3.2.

$$LCHS = \frac{C_{NPC}}{\sum_n^N i_D M_{H_2}} \quad (3.2)$$

Where C_{NPC} is the net present cost, M_{H_2} is the cumulative hydrogen storage over time, n is the year of its use, N is the system lifetime and i_D is the discount rate [4]. The C_{NPC} is calculated with Equation 3.3.

$$C_{NPC} = C_{CapEX} + \sum_n^N i_D (C_{OpEx}) \quad (3.3)$$

Where C_{CapEX} is the Capital Expenditure (CAPEX) of the system and C_{OpEx} is the Operational Expenditure (OPEX) of the system.

The LCHS of different storage methods are displayed in Figure 3.11.

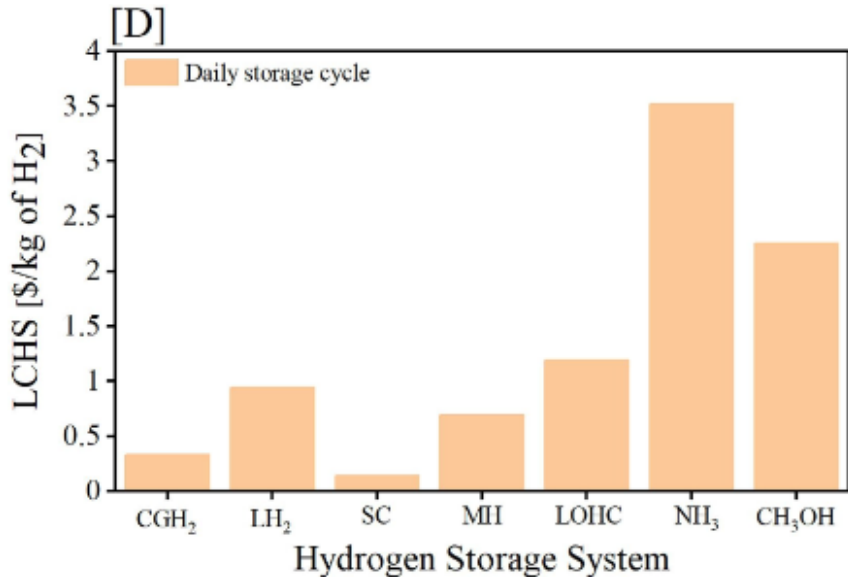


FIGURE 3.11: Levelized cost of multiple hydrogen storage methods [4].

The different methods shown in Figure 3.11 are: CGH₂ (compressed hydrogen), LH₂ (liquid hydrogen), SC (salt cavern), MH (metal hydride), LOHC, NH₃ (ammonia) and CH₃OH (methanol). It shows that compressed hydrogen storage is one of the cheapest forms of hydrogen storage. The only one that costs even less is the use of salt caverns. Using salt caverns would decrease the cost of storage significantly, but such a natural phenomenon needs to be available in the vicinity of the hydrogen production plant, and is more used for long-term storage.

3.4 Simulation Scenarios: Technical Performance

With the model established, multiple simulation scenarios can now be defined. The main goal of this study is to evaluate both the technical and economic performance of the hydrogen storage system proposed by ROGER Energy, and come up with design optimizations.

To achieve this, the baseline scenario is first constructed by simulating the system as proposed by ROGER Energy. This baseline will then be compared with alternative scenarios in which selected key parameters are varied. By analyzing the impact of these variations, the influence of each parameter on system performance can be assessed, and potential improvements to the proposed design can be identified. To first identify the technical performance of the system, a large number of "smaller" simulations will be performed of 90 days. This is deemed adequate time to give insight into the system's operations.

In the following sections, the key parameters and their respective values are described.

3.4.1 Pressure

The first key parameter to be varied is the storage pressure. The maximum allowable pressure is limited by the strength of the tank material. Since the tanks are of Type I design, the absolute upper limit is approximately 200 bar. Operating directly at this limit poses safety concerns; therefore, in this study, the maximum considered pressure is set to 180 bar. The minimum pressure is limited to 40 bar, corresponding to the hydrogen production pressure, and may be increased up to 70 bar.

The influence of the storage pressure is therefore assessed by evaluating combinations of minimum and maximum pressures. The minimum pressure is varied from 40 bar to 70 bar, in steps of 10 bar, while the maximum pressure is varied from 100 bar to 180 bar, in steps of 20 bar. This results in a set of pressure combinations that together capture both the effect of raising the maximum allowable pressure and of decreasing the minimum operating pressure. This way, the individual and combined influence of the storage pressures on the system performance can be systematically compared.

As discussed in Chapter 3.1.3, the compressors can operate up to a maximum temperature of 85 °C. To maintain the temperature below this limit, multiple compression stages with intercooling between each stage are required. For the compressors used to fill the storage, the maximum pressure is the determining factor. At a maximum pressure of 100 bar, two compression stages are sufficient, while higher pressures require three stages. Conversely, for the compressors used to empty the storage, the minimum pressure is critical. When the minimum pressure is 70 bar, two stages are needed; if the pressure drops below this value, three stages become necessary.

3.4.2 Logistical Capacity

The next key parameter is the outgoing logistical capacity, which determines the maximum rate at which hydrogen can be withdrawn from the storage system. If the logistical capacity is too low, hydrogen accumulates in the tanks, eventually leading to production curtailment once the storage is full. Ensuring sufficient outbound capacity is therefore essential for maintaining effective operation of the system.

In the baseline design, the system includes five filling stations, each with a maximum flow rate of 90 kg/h, resulting in a total capacity of 450 kg/h. To evaluate the impact of higher logistical capacity, simulations are conducted with the number of filling stations increased to six and seven. Each additional station adds 90 kg/h of capacity, leading to total capacities of 540 kg/h and 630 kg/h. These three scenarios, will be combined with the pressure configurations to get a good understanding of the trend and determine the adequate storage capacity for each scenario.

3.4.3 Operational Days

The final key parameter considered is the number of operational days per week. While hydrogen production occurs continuously on a 24/7 basis, the filling stations are not operated throughout the entire week and function at reduced flow rates during the night shift. This mismatch causes hydrogen to accumulate in the storage system during inactive periods, particularly over weekends. If storage remains full for an extended period, production may need to be reduced or stopped entirely.

To assess the impact of operational days, three scenarios are evaluated:

1. two days of station inactivity per week (baseline, 5 operating days)
2. one day of station inactivity per week (6 operating days)
3. continuous operation with no inactive days (7 operating days).

Again, with these scenarios, they will be combined with the pressure configuration simulations to determine the optimal storage capacity for these scenarios.

3.5 Simulation Scenarios: Economic Performance

After running the simulations for the technical performance, an optimized new scenario was chosen based on the KPIs. This new scenario was then compared to the originally proposed scenario that ROGER designed. It was compared using economic KPIs like the LCHS. From this, a recommendation will come forth as to what action needs to be undertaken to improve the overall performance of the storage.

3.6 Key Performance Indicators: Technical Performance

To compare simulation scenarios in a consistent manner, a set of Key Performance Indicators (KPIs) is defined to capture the technical feasibility of the hydrogen storage system integrated with the production plant.

The KPIs used for the technical feasibility analysis are:

- **Delivery delay** [min/truck]
- **Realized production** [%]
- **Outgoing hydrogen** [kg]

The delivery delay counts the number of iterations that a truck was ready, but there was not enough hydrogen available. The KPI then determines how many minutes on average a truck needs to wait for its hydrogen. The realized production will divide the actual hydrogen production by the potential production (the hydrogen production that could have been, if not limited by the storage). Finally, the outgoing hydrogen is the amount of hydrogen that has been delivered to the trucks and has thus been sold.

3.7 Key Performance Indicators: Economic Performance

For the final comparison between the original and the optimized scenarios, both technical and economic factors are considered. The technical KPIs are identical to those used for the technical performance analysis. To evaluate economic performance, the following KPIs are used:

- Energy consumption (kWh/kg output)
- Energy costs (€/kg output)
- Levelized Cost of Hydrogen Storage (LCHS) (€/kg output)

The formula for the LCHS is given in Chapter 3.3 in Equation 3.2. To calculate the LCHS, CAPEX and OPEX of the systems is needed over the lifetime of the project. They are partially based on the business case that ROGER has provided.

The CAPEX includes the following components:

- Underground hydrogen storage tanks
- Compressors for charging (filling) the storage
- Compressors for discharging (emptying) the storage
- Filling stations

The costs of these components are estimated using data from the ROGER business case. Per scenario, the total CAPEX can differ. The costs for the underground storage tanks will not vary, as the volume is kept the same, and same material is assumed (Type I). An increase in the number of filling stations will cause an increase in the total cost of the filling stations, but this increase is assumed to be linear. Finally, the costs for the compressors can also vary, as a higher maximum pressure requires one more compressor stage. The same applies for a lower minimum pressure. Adding more compressor stages increases the cost and the complexity, as it requires an additional cylinder, valves, and intercooler. The increase in cost per stage is assumed to be 20% of the original CAPEX [32].

In addition to CAPEX, the OPEX is also calculated, consisting of two primary components:

- Maintenance costs
- Electricity costs for compression and cooling

These are the main contributors to the operational costs of the hydrogen storage system. Equation 3.3 also includes a decommission cost; however, this is disregarded in this calculation. Maintenance costs are estimated as a percentage of CAPEX. The maintenance cost of compressors is approximately 4% of CAPEX [33], for the filling stations it is assumed to be 3% of CAPEX, and for the underground storage tanks 1.5% of CAPEX [34]. The electricity costs for compression and cooling are dynamically calculated within the model, using the dynamic energy price. The energy requirement for each iteration is determined and multiplied by the corresponding electricity price at that time step.

Personnel costs were also considered; however, these are difficult to isolate since personnel operate the entire plant rather than the storage system alone. Therefore, personnel costs are excluded from the current economic assessment.

Finally, the plant must achieve a certain hydrogen output to be economically viable. The required hydrogen output for economic feasibility is taken from the ROGER business case and will be further discussed in the *Results* section.

Chapter 4

Results & Discussion

This chapter presents the results of the techno-economic performance analysis. It discusses the effects of varying key parameters on the technical and economic performance of both the current design by ROGER and the proposed alternative scenarios. Before analysing these results, the model was first verified to ensure that it accurately follows the intended design, as described in the following section.

4.1 Model Verification

The system that is modelled in this study is based on a specific proposed system, designed by ROGER Energy, and which is still in development. Therefore, direct validation against experimental or operational data was not possible. Instead, model verification was performed to ensure that the implemented system operates in accordance with fundamental physical principles and exhibits behaviour consistent with theoretical expectations.

To verify the operational behaviour of the system, simulation results for hydrogen output and storage level over the course of one representative week are presented. These simulations were carried out under standard operating conditions, with a maximum pressure of 100 bar and a minimum pressure of 40 bar.

The model should reproduce the intended operational control behaviour as designed. This means it should correctly apply the input parameters, including hydrogen production rates and energy prices, and produce the expected hydrogen output during different operational periods, such as start-up and the night shift. Furthermore, the model should ensure that the total net mass in storage accurately reflects the cumulative inflow and outflow of hydrogen, confirming that the mass balance is consistent with the defined control logic. Plots for the hydrogen output and the total mass in the storage over time are displayed in Figure 4.1 and 4.2.

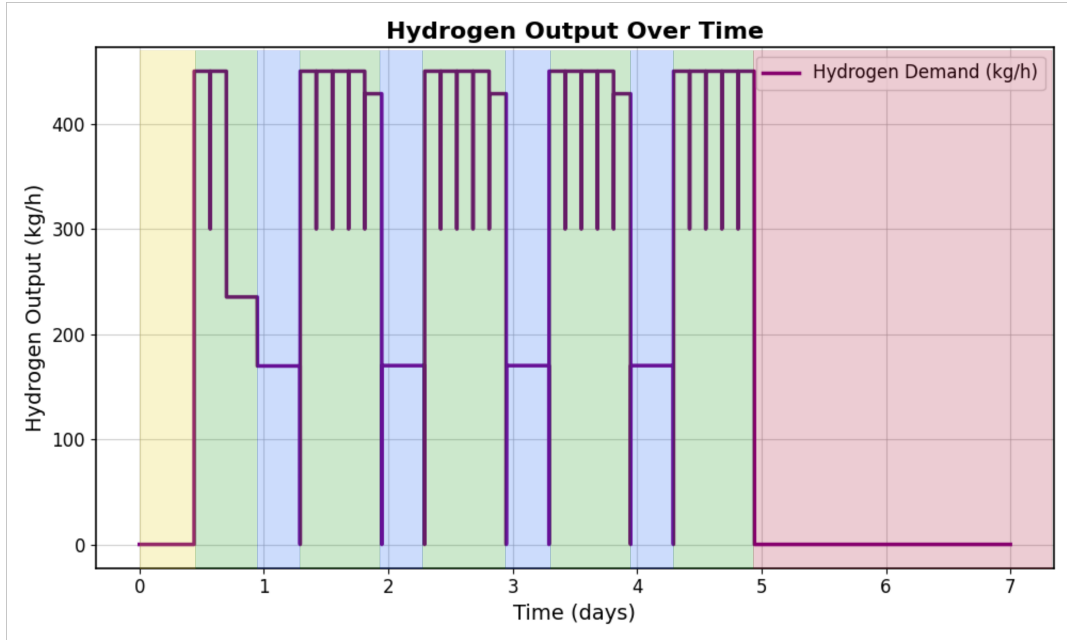


FIGURE 4.1: The outgoing hydrogen of a system during the second week under normal conditions and a configuration of 100-40. Simulation phases: start-up phase (yellow area), day shifts (green area), night shift (blue area), and non-operating days (red area).

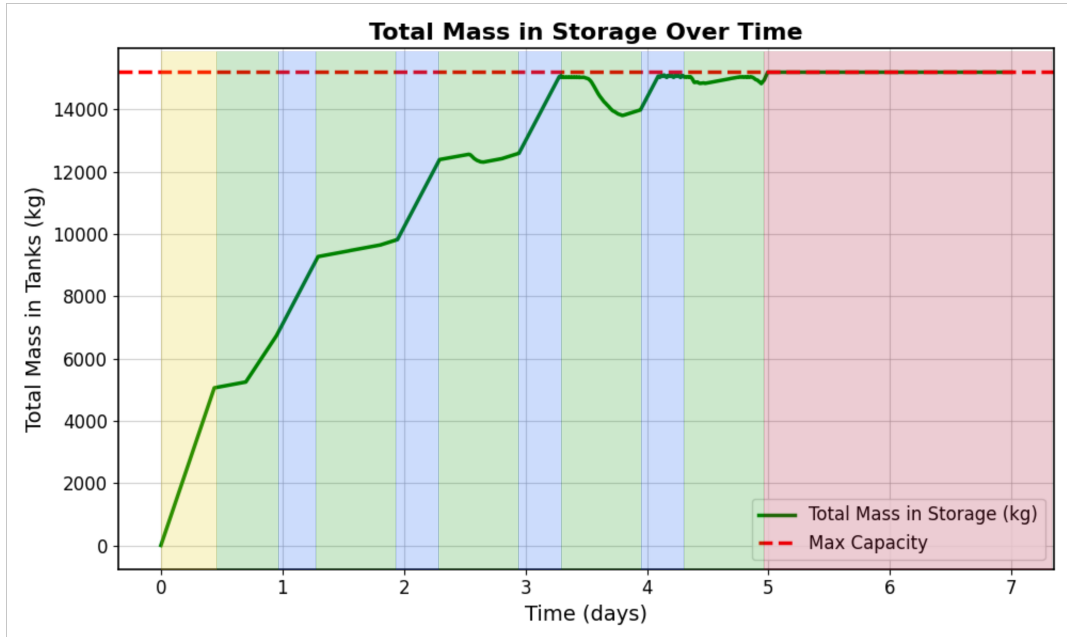


FIGURE 4.2: The total net mass in the storage during one week using standard conditions and a pressure configuration of 100-40. Simulation phases: start-up phase (yellow area), day shifts (green area), night shift (blue area), and non-operating days (red area).

Figure 4.1 illustrates the outgoing hydrogen flow during one week of simulation. At the beginning of the simulation, the system shows no hydrogen output, which correctly represents the start-up phase (yellow area). During this period, the system must first reach a minimum operational level before delivery can commence. Once this level is achieved, the output rapidly increases to its maximum value, corresponding to the first day shifts (green area).

After several hours, the output decreases in two steps: the first step maintaining a higher flow than the second. The second step represents the night-shift operation (blue area), while the first step reflects a brief mismatch between the day and night shift transitions. The night shift is characterized by reduced output, as truck filling occurs overnight, reducing the flow rate. In subsequent days, the magnitude of this intermediate step decreases, indicating improved synchronization between day and night shift operations. At the end of the week, the hydrogen output returns to zero, marking the start of the non-operational weekend period (red area).

Figure 4.2 shows the total net hydrogen mass in storage over the course of one simulated week. The same time periods indicated by the coloured areas in Figure 4.1 are used here for comparison. At the start of the simulation, the storage level increases linearly, representing the start-up phase during which hydrogen is accumulated before delivery begins.

Following this phase, the total mass continues to rise at varying rates. A moderate increase corresponds to the transition into the first day shift and subsequent step decrease in output, after which a steeper rise marks the beginning of the night-shift period. Over the following days, alternating periods of smaller and larger increases appear, reflecting fluctuations in hydrogen production (see Figure 4.3). Toward the end of the week, the storage level reaches its maximum and remains constant, indicating the non-operational weekend period when no hydrogen is withdrawn.

Besides verifying the system's output, the input data also need to be checked. The model uses two main inputs: hydrogen production and the dynamic electricity price. Although data for both are available for the entire year, a one-week period is shown here to give a clear overview (Figure 4.3 and 4.4).

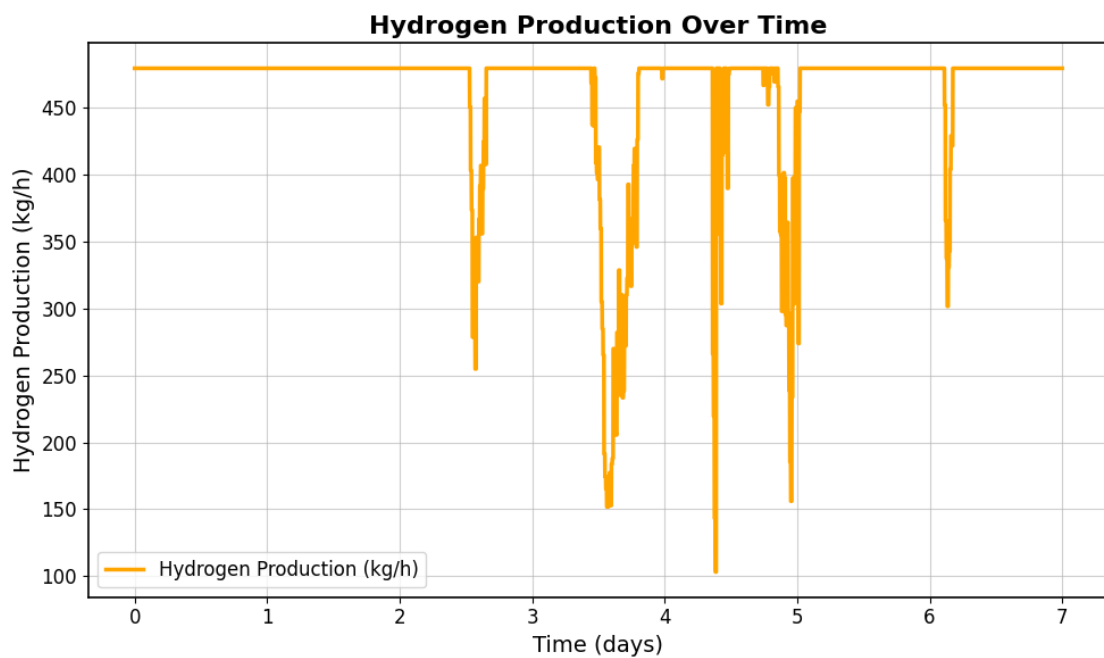


FIGURE 4.3: The hydrogen production for a simulation of one week.

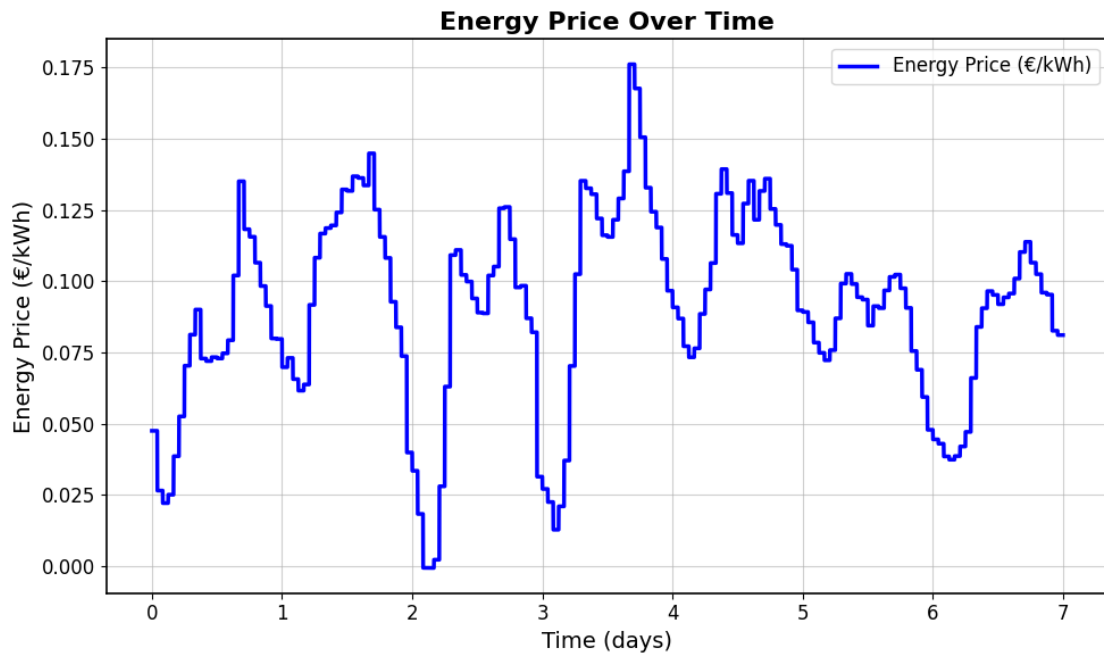


FIGURE 4.4: Energy price data during a one week simulation.

The hydrogen production profile (Figure 4.3) comes from the PEM and SOEC electrolyzers. As described in Chapter 3.1.1, the total production capacity is set at 19.4 MW, which equals a maximum hydrogen output of 480 kg/hour. This corresponds to the maximum value in Figure 4.3. The fluctuations in the hydrogen production are a direct result of varying wind speeds. When the wind speed drops significantly, the wind turbines generate less than 19.4 MW. This leads to reduced hydrogen production.

The electricity price data (Figure 4.4) shows a clear fluctuating pattern, with lower prices occurring during nighttime hours and higher prices during the daytime. In addition, price variability is reduced during the weekend compared to weekdays. Since only hourly data is available, the electricity price is assumed to remain constant within each hourly interval.

For the final verification of the system, a mass balance was calculated over the simulation period, as shown in Equation 4.1:

$$E_{\text{mass}} = M_{\text{prod}} - M_{\text{demand}} - M_{\text{storage}} - M_{\text{unhandled}} \quad (4.1)$$

Where E_{mass} is the mass balance error, M_{prod} is the cumulative hydrogen production over the total simulation period, M_{demand} is the cumulative hydrogen demand, M_{storage} is the final total mass in the storage, and $M_{\text{unhandled}}$ is the unhandled hydrogen.

The resulting final mass balance error equals zero, confirming that the model conserves mass correctly.

4.2 Scenario Testing: Technical Performance

The technical performance of the system with varying key parameters will indicate the influence they have on the system. Three key parameters have been varied and compared using three KPIs. All the simulations in this section have been performed over a period of 90 days, and using multiple configurations of the minimum and maximum pressures (pressure-configuration). The results of these simulations and their comparisons can be found in the following subsections.

4.2.1 Pressure Configuration

The size of the system is partially determined—together with the storage volume—by its pressure configuration, consisting of a minimum and maximum pressure. The minimum pressure can range from 70 to 40 bar, while the maximum pressure can vary between 100 and 180 bar. All 20 possible configurations were simulated over a period of 90 days. All other key parameters were kept constant: five filling stations, five operational days, and a storage volume of 3221 m^3 (specified by ROGER). The outcomes of these simulations are displayed in Figure 4.5.

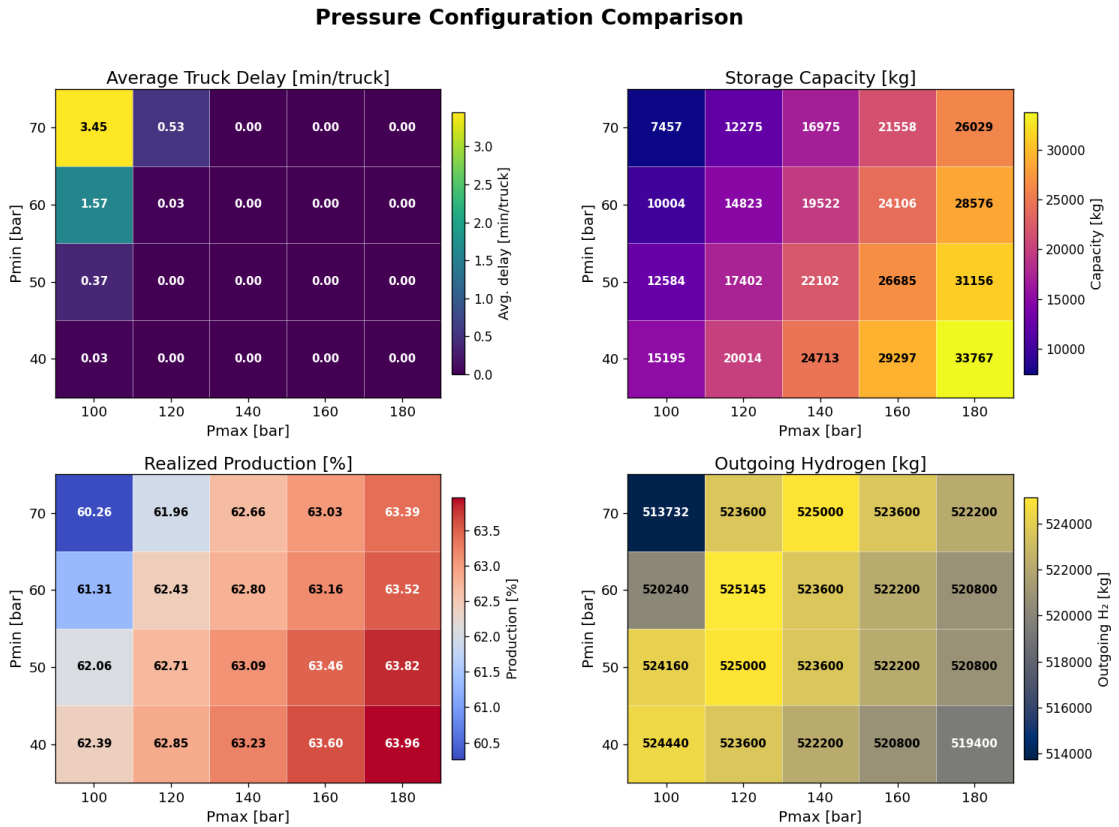


FIGURE 4.5: Comparison of all pressure configurations, using standard conditions for the system (5 filling stations and 5 operational days).

The first KPI evaluated is the *storage capacity*. Pressure and storage capacity are directly related: lowering the minimum pressure or increasing the maximum pressure results in a larger usable capacity. As shown in the top right plot in Figure 4.5, the storage capacity increases steadily as the minimum pressure decreases and/or the maximum pressure increases, which aligns with expectations.

To determine which capacity is sufficient for the system, the next KPI evaluated is the *delivery delay*, that represents the average additional waiting time per truck when insufficient hydrogen is available for refuelling. The values for this KPI per pressure configuration are shown in the top left plot in Figure 4.5. In that plot, several configurations exhibit a non-zero delay. These are primarily configurations with a maximum pressure of 100 bar, and a few with 120 bar. A non-zero delay indicates that the storage is too small to buffer fluctuations in hydrogen production. During periods of reduced production, the available hydrogen becomes insufficient to meet demand, causing trucks to wait for refuelling.

The next KPI is the *realized production*, defined as the ratio of actual hydrogen production to potential production. The difference between the two arises when the storage reaches its maximum capacity, forcing production to stop to prevent hydrogen venting temporarily. A higher realized production indicates more hydrogen being produced and possibly sold, improving overall performance. As seen in the bottom left plot in Figure 4.5, the realized production increases as the storage capacity increases. However, it increases only slightly, by a couple of percentage points, while the storage capacity increases significantly more.

To provide additional context, the bottom right plot in Figure 4.5 shows the total amount of hydrogen delivered over the 90-day period for each pressure configuration. The total hydrogen delivered remains relatively constant for most configurations, except for 100–70, which shows reduced performance. Interestingly, the delivered amount decreases slightly for configurations larger than 120–50 or 140–70 bar. This effect is caused by system start-up behaviour: larger storages require more time to fill before fuelling operations can begin. The realized production nonetheless continues to increase slightly with larger capacities because the additional stored hydrogen compensates for the reduced early deliveries.

By evaluating the system using these KPIs, it can be concluded that pressure configurations 100–70, 100–60, 100–50, and 120–70 bar are undersized (considering a volume of 3221 m^3), as they fail to adequately buffer fluctuations in hydrogen production and lead to delivery delays. Meanwhile, increasing the pressure range beyond 120–50 or 140–70 bar yields diminishing returns: while it increases the stored hydrogen, it does not result in additional hydrogen delivered to customers. If the preferred operating pressure corresponds to one of the pressure configurations which is deemed undersized, this delay can be mitigated by increasing the storage volume of the system. The optimal pressure configurations correspond to a storage capacity of approximately 17,000 kg of hydrogen (in a system with five filling stations and five operational days). Therefore, in the case of ROGER’s design, the volume of the system should be increased accordingly to achieve the best performance within the analysed pressure range.

4.2.2 Logistical Capacity

The proposed system includes five filling stations, each with a maximum flow rate of 90 kg/h, resulting in a total capacity of 450 kg/h. The previous section analyzed a system with five filling stations. To explore the effect of expanding the system's outgoing (logistical) capacity, additional simulations were conducted with six and seven filling stations, respectively. The impact of increasing the number of filling stations on the average truck delay is illustrated in Figure 4.6.

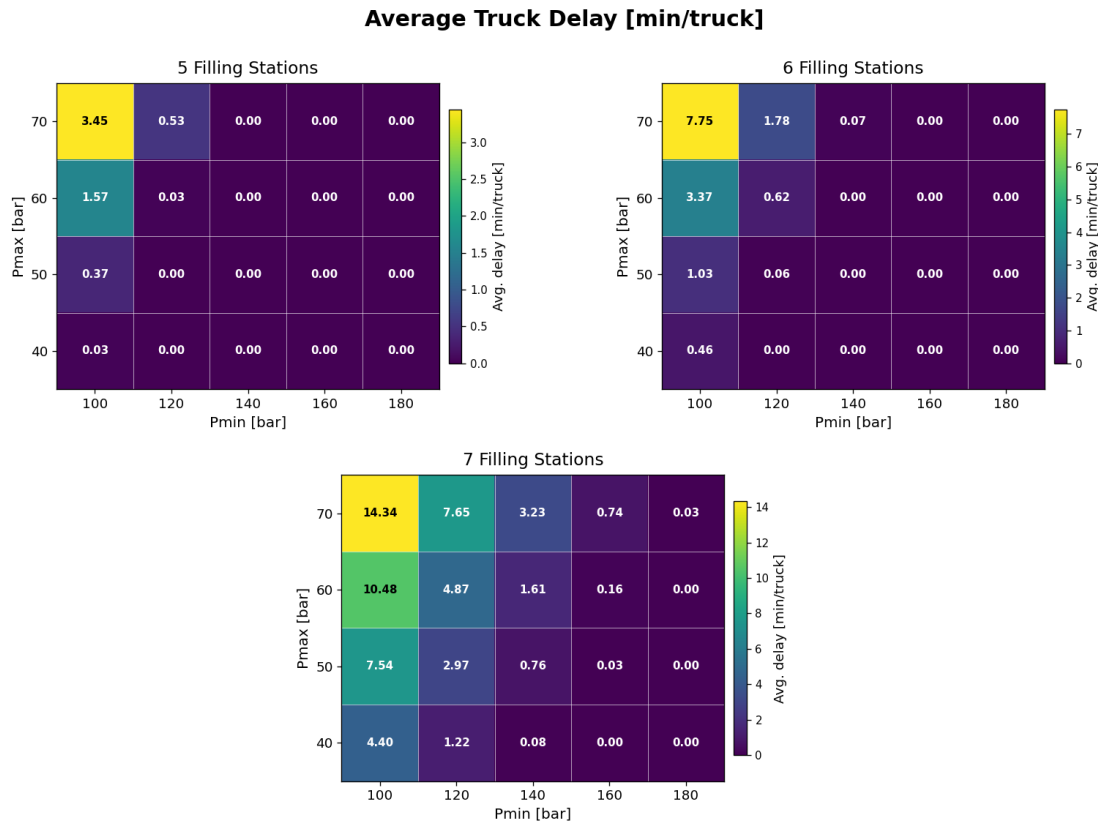


FIGURE 4.6: The average delay per truck per pressure configuration, in a system with five, six, and seven filling stations.

When the number of filling stations increases to six, the top right plot in Figure 4.6 shows that the average delay per truck rises for the lower pressure configurations compared to the system with five filling stations (top left plot in Figure 4.6). The area representing configurations with zero delay shifts to the right, indicating that fewer configurations have sufficient capacity to handle the production fluctuations. At six filling stations, a maximum pressure of 100 bar is insufficient regardless of the minimum pressure, while a maximum pressure of 120 bar is only effective at low minimum pressures.

When the number of filling stations is further increased to seven, the bottom plot in Figure 4.6 shows an even greater increase in delay across all configurations. Only the higher-pressure configurations exhibit zero average delay values. Specifically, only the pressure configurations with a maximum pressure of 180 bar, as well as the 160–40 configuration,

achieve an average delay per truck of zero. This indicates that the storage capacity must be significantly increased compared to the current setup to effectively handle the fluctuations in hydrogen production, due to the increased hydrogen output rate.

In addition to the impact on average truck delay, an increase in the number of filling stations also affects the realized hydrogen production. The realized production for systems with five, six, and seven filling stations, across the different pressure configurations, is shown in Figure 4.7.

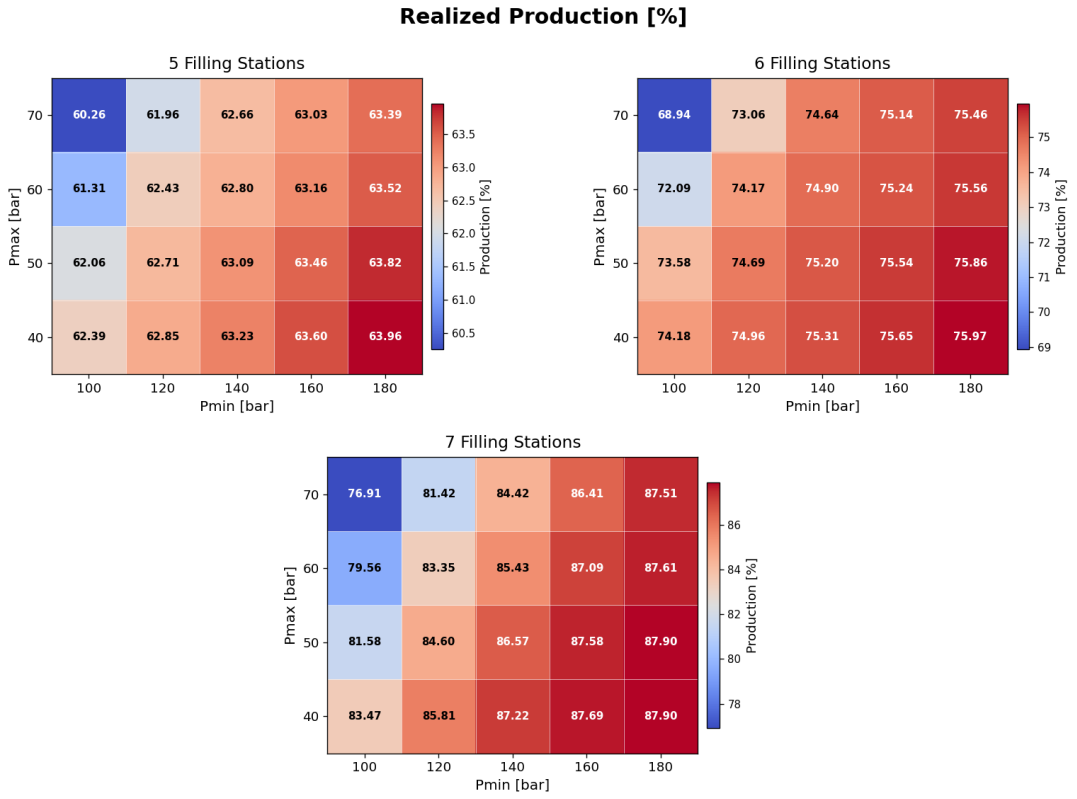


FIGURE 4.7: The realized production (%) per pressure configuration, in a system with five, six, and seven filling stations.

For a system with six filling stations, the top right plot in Figure 4.7 shows that the realized production increases significantly compared to the system with five filling stations (top left plot in Figure 4.7). The realized production range rises from 60.26–63.96% to 68.94–75.97%. The higher outgoing capacity leads to greater system depletion during operational days, allowing for increased hydrogen intake during non-operational days and thereby reducing periods when the storage is full. This effect becomes even more pronounced when the number of filling stations increases to seven, where the realized production range further rises to 76.91–87.90%.

Finally, the total outgoing hydrogen for the systems with five, six, and seven filling stations is shown in the plots in Figure 4.8.

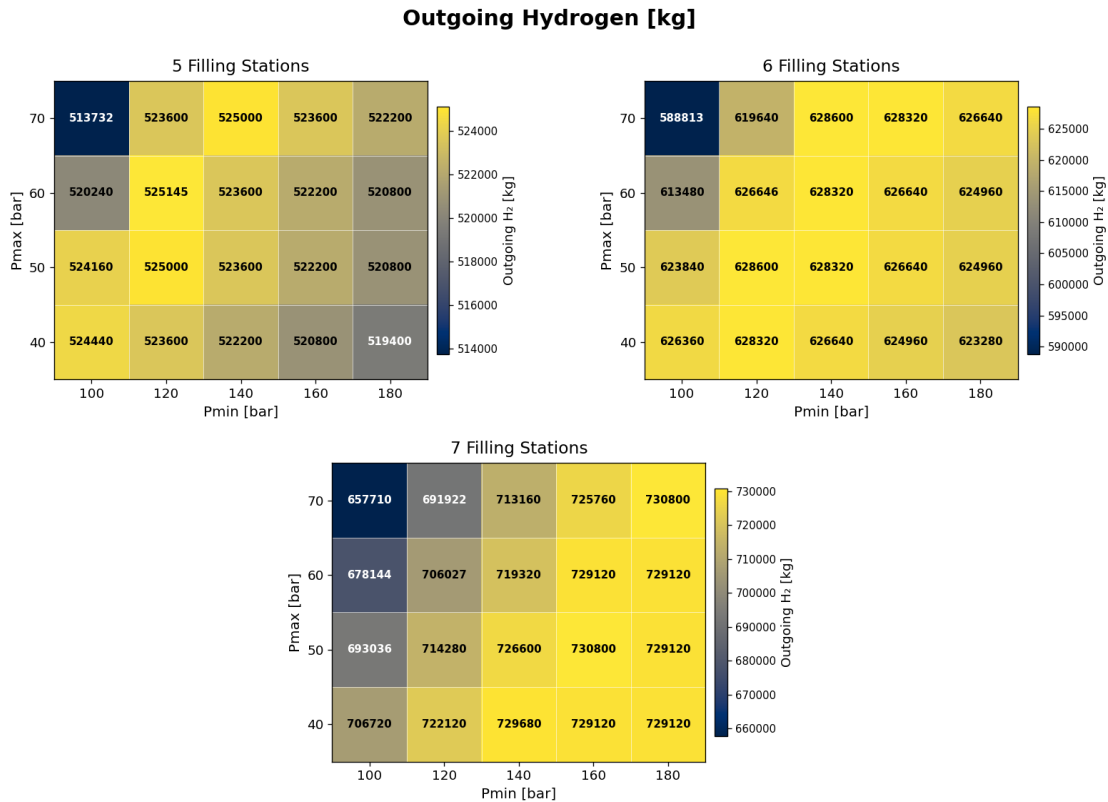


FIGURE 4.8: The outgoing hydrogen per pressure configuration, in a system with five, six, and seven filling stations.

The top right plot in Figure 4.8 shows that, for a system with six filling stations over a period of 90 days, the maximum hydrogen output reaches 628,600 kg. This maximum is achieved at the pressure configurations 120-50 and 140-70. Increasing the pressures beyond these levels does not provide additional benefits and instead leads to higher system wear and increased safety risks. For the system with seven filling stations (bottom plot of Figure 4.8), the maximum hydrogen output is achieved at 160-50 and 180-70. However, lower pressure configurations like 140-40 and 160-60 have similar output values (only slightly less).

Increasing the number of filling stations enhances both realized production and total hydrogen output by keeping storage levels lower, which allows more hydrogen to be stored during non-operational periods. However, this comes at the cost of higher system depletion and a need for larger storage capacity. Expanding to six and seven filling stations are both technically feasible and are significant improvements in terms of hydrogen output. However, this does also require a significant increase in storage capacity to keep operational stability.

4.2.3 Operational Days

One of the limiting factors of the proposed system is the non-operational period during weekends, while hydrogen production is maintained continuously throughout the week. During these non-operational days, the filling stations are unmanned, preventing any hydrogen outflow. As observed in the pressure configuration simulations, this results in a lower realized production, since the storage capacity fills up quickly during these periods.

To assess the impact of extended operation, the same pressure configurations were simulated assuming six and seven operational days per week. The effects on the average truck delay for these scenarios are presented in Figure 4.9.

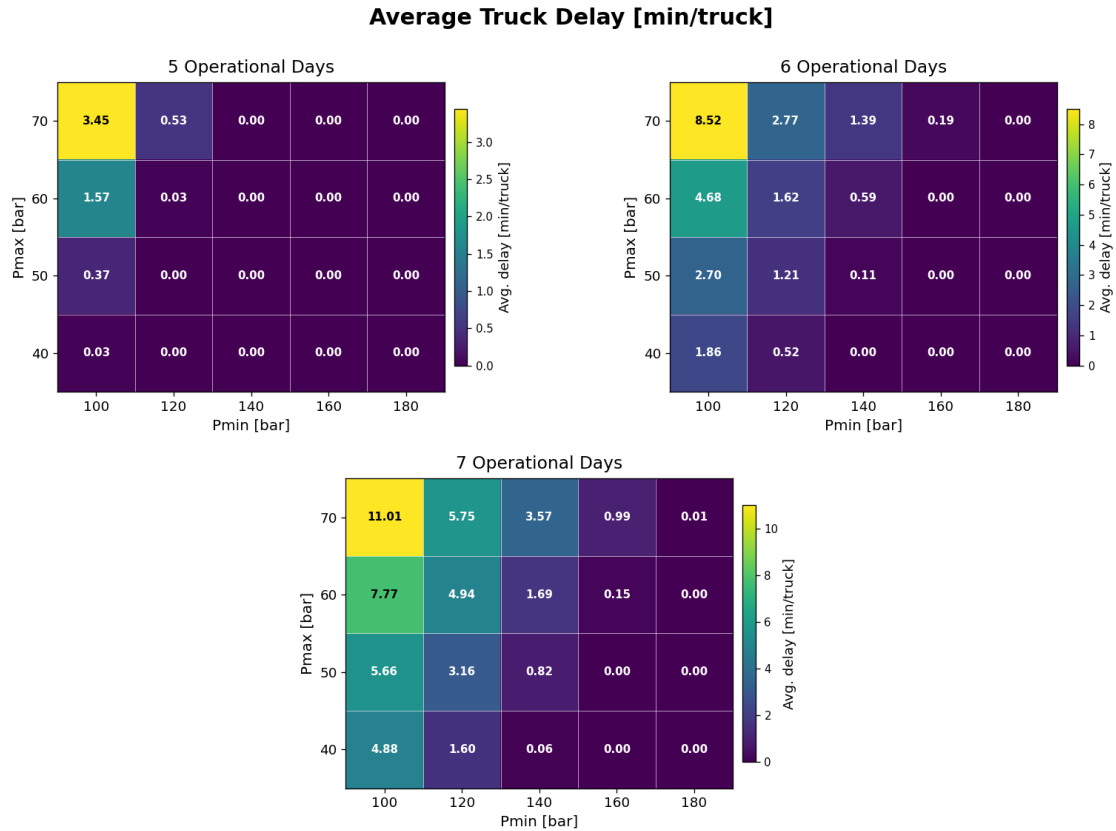


FIGURE 4.9: The average delay per truck per pressure configuration, in a system with five, six, and seven operational days per week.

As shown in the plots in Figure 4.9, the average delay increases for the lower pressure configurations, while the configurations with zero delay shift to the right compared to the system operating with five days. At six operational days, the first configurations achieving zero average delay are 140–40 and 160–60. When extended to seven operational days, a zero delay is observed at 160–50 and 180–60. To have operations with minimal delay, a significant increase in storage capacity is needed.

The next KPI is the realized production, which is plotted for five, six, and seven operational days in Figure 4.10.

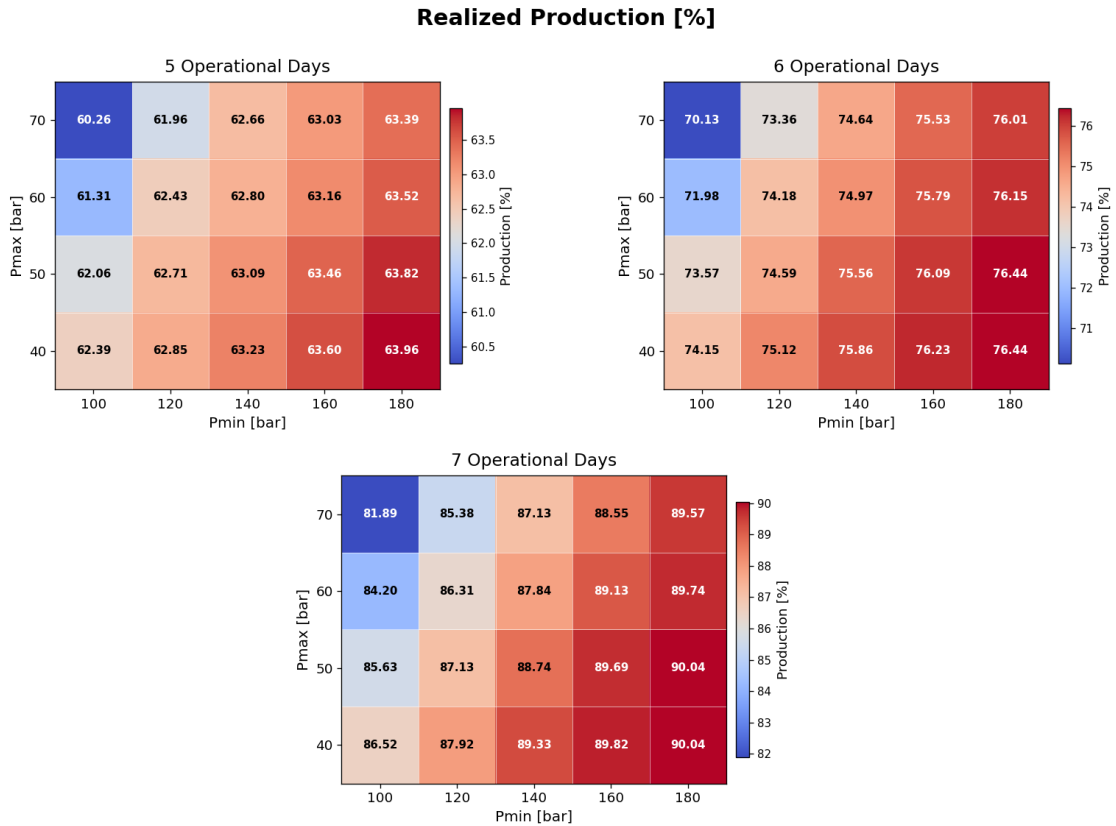


FIGURE 4.10: The realized production per pressure configuration, in a system with five, six, and seven operational days per week.

In the system with six operational days (top right plot in Figure 4.10), the realized production increases significantly compared to a system operating five days per week, across all pressure configurations. A system with five operational days achieves a realized production range of 60.26–63.96%, whereas extending to six operational days increases this range to 70.13–76.44%. For a system operating seven days per week, the improvement is even more pronounced, with realized production ranging from 81.89–90.04%.

The final comparison is made via the outgoing hydrogen, which is plotted in Figure 4.11.

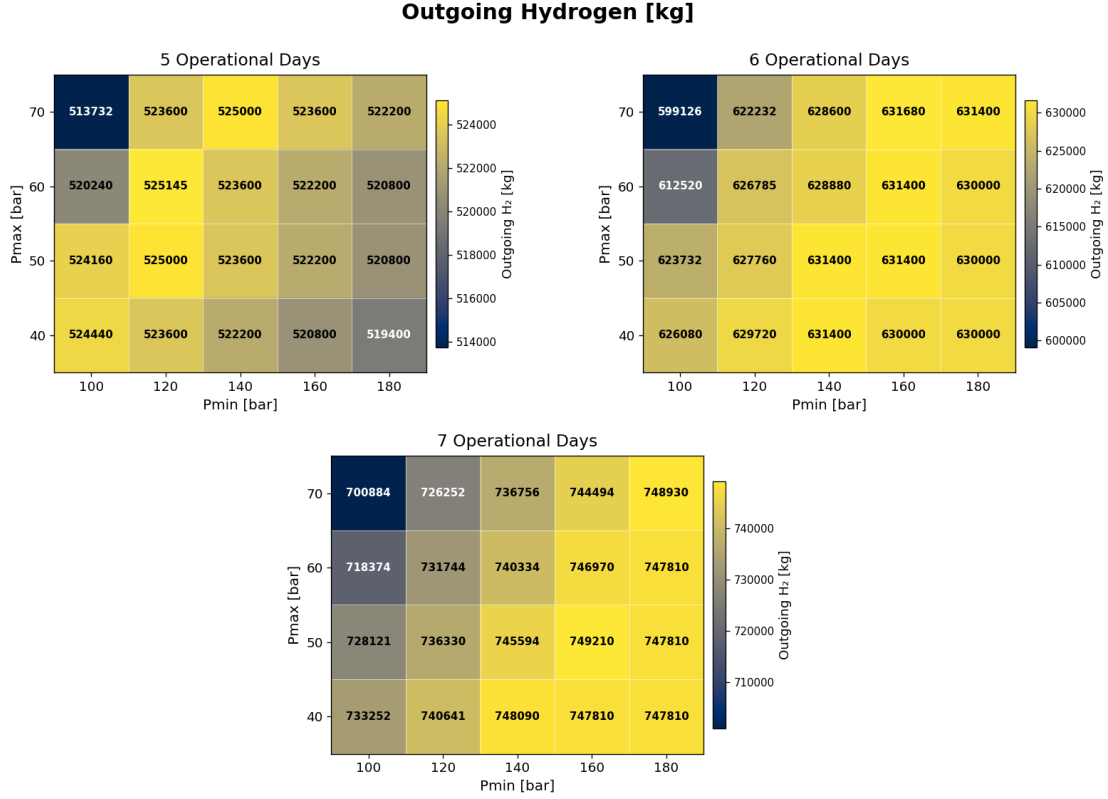


FIGURE 4.11: The outgoing hydrogen per pressure configuration, in a system with five, six, and seven operational days per week.

The top right plot in Figure 4.11 shows that the optimal pressure configuration for six operational days is 160-70, achieving a hydrogen output of 631,680 kg over a 90-day period. However, lower pressure configurations have only a slightly less output, with 140-50 having an output of 631,400 kg. At higher pressure configurations, the output is slightly lower due to longer start-up times. For seven operational days (bottom plot), the highest hydrogen output is obtained at the 160-40 configuration, reaching 746,970 kg in 90 days. Similarly, at higher pressure configurations, the output decreases as a result of extended start-up durations.

Extending the number of operational days increases the utilization of the available storage capacity and enhances overall hydrogen production. However, similar to the effect of adding more filling stations, this improvement also introduces greater operational instability. To mitigate this, the storage capacity must be adequately expanded. When the number of operational days per week is increased in combination with a sufficient storage capacity, the hydrogen output of the system improves substantially while maintaining a stable operation.

4.2.4 Combination

From the previous simulations, it became evident that both increasing the number of filling stations and the number of operational days per week were beneficial for the performance of the system. Therefore, additional simulations were performed that combine these two improvements: a system with six filling stations operating six days per week. The results of this combination are shown in Figure 4.12.

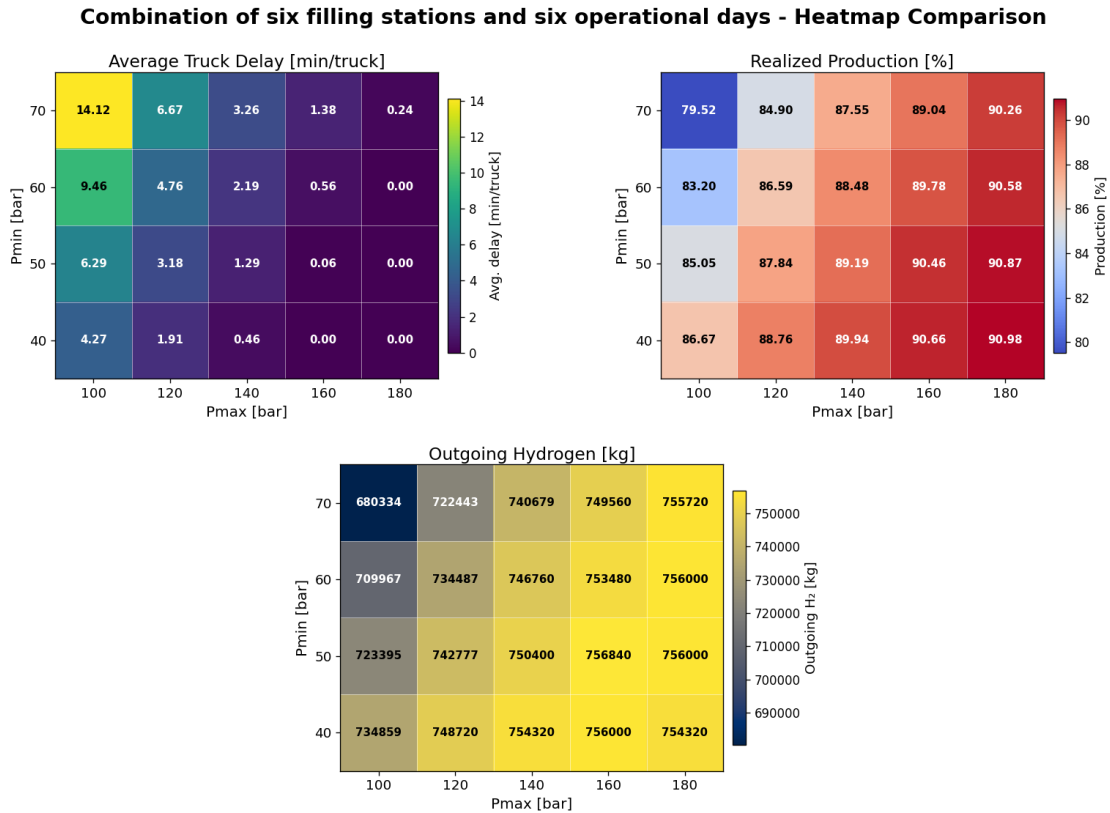


FIGURE 4.12: Comparison of all pressure combinations for a system with six filling stations and six operational days.

The combination of six filling stations and six operational days further increases the output capacity of the system. Consequently, both the realized production and total hydrogen output rise compared to systems with six filling stations and six operational days separately. The optimal pressure configuration is 160-50, with a hydrogen output of 756,840 kg, which is the highest across all scenarios. The increase in output does come with a requirement to increase the maximum pressure to 160 bar, to keep the average delay low.

4.2.5 Optimized scenario

Based on all previous simulations, a new optimized scenario has been selected and compared with the original setup proposed by ROGER Energy. Two criteria determined the optimized scenario: minimizing the average delay per truck and maximizing the hydrogen output. The system configuration that best met these criteria was the combination of six filling stations and six operational days, at a pressure configuration of 160-50.

A system operating seven days per week was also considered (although it resulted in a slightly lower total hydrogen output). However, this scenario was not selected due to practical and logistical constraints. In particular, truck operations are generally limited on Sundays, as most transport companies either do not schedule drivers or face restrictions related to working hours and driver availability.

Therefore, the input values for the original and optimized systems are given in Table 4.1.

TABLE 4.1: Input values for the original and optimized system setups.

Parameter	Original design	Optimized design
Volume [m ³]	3,221	3,221
Maximum pressure [bar]	100	160
Minimum pressure [bar]	70	50
Number of filling stations	5	6
Operational days	5	6
Compressor filling stages	2	3
Compressor emptying stages	2	3

For both simulations, the volume is kept the same. The number of filling stations and operational days are both increased to six. The pressure configuration for the current system design is 100-70, and for the optimal design is 160-50. As discussed in Chapter 3.4.1, increasing the maximum pressure above 100 bar requires an additional compressor stage to fill the storage. The same applies when the minimum pressure is lowered to below 70 bar.

The technical results of the one year simulations with these inputs are given in Table 4.2.

TABLE 4.2: Technical output values for the original and optimized system designs.

Parameter	Original design	Optimized design
Storage capacity (kg)	7,457	26,685
Outgoing hydrogen (kg)	1,960,053	2,988,419
Total unhandled (kg)	1,322,995	276,169
Final mass in storage (kg)	7,366	25,827
Average delay (min/truck)	10.06	3.37
Total delay (hours)	1,172	599
Production potential (kg)	3,290,414	3,290,414
Actual production (kg)	1,967,418	3,014,245
Realized production (%)	59.79	91.61

The results in Table 4.2 clearly indicate that the optimized design performs significantly better than the original. The hydrogen output increased by 52% (from 1,960,053 to 2,988,419 kg), while the average delay per truck decreased from 10.06 to 3.37 minutes. Furthermore, the realized production rose from 59.79% to 91.61%, demonstrating a more efficient use of the available production capacity.

The increase in hydrogen output is particularly relevant in relation to the project's production targets. According to the business case of ROGER Energy, the total expected hydrogen production is 52.2 million kg over a 20-year project lifetime. This corresponds to approximately 2.6 million kg per year. This annual target is achieved by the optimized design (2.99 million), whereas the original setup falls short (1.96 million).

4.3 Scenario Testing: Economic Performance

The new optimised design (identified in the previous section) will be compared to the design that ROGER Energy currently envisions to identify possible improvements in economic performance. The comparison covers the original system, with a pressure configuration of 100-70, and the optimized system, which has a pressure configuration of 160-50. All input values can be seen in Table 4.1.

4.3.1 Energy Consumption and Costs

An important factor in evaluating the economic performance of the storage system is its energy consumption and the associated energy costs. The results for both the original and optimized designs are shown in Table 4.3.

TABLE 4.3: Energy performance comparison for the original and optimized system designs.

Parameter	Original design	Optimized design
Outgoing hydrogen (kg)	1,960,053	2,988,419
Total energy consumption (MWh)	4,271.81	7,138.97
Energy consumption (kWh/kg output)	2.18	2.39
Energy costs (€)	411,443.59	640,150.11
Energy costs (€/kg output)	0.210	0.214

The total energy consumption increased from 4,272 MWh in the original system to 7,139 MWh in the optimized system. When normalized per kilogram of hydrogen output, the optimized design is slightly less energy efficient (2.39 kWh/kg compared to 2.18 kWh/kg). This decrease in efficiency is likely caused by the larger pressure range in the optimized setup, which requires additional compression energy. Another contributing factor is the increased storage capacity: since the tank is nearly full at the end of the simulation, part of the stored hydrogen is already compressed but not yet counted as output, still contributing to the total energy consumption.

Despite this higher energy demand, the energy costs per kilogram of hydrogen only increase marginally (from 0.210 to 0.214 €/kg). This smaller difference is caused by going from five to six operational days. The difference between the two is the inclusion of Saturday. The energy prices on Saturday are, on average, lower than on weekdays (Monday to Friday). As a result, even though total energy use rises, the overall cost increase remains limited.

Overall, the original design remains slightly more energy efficient and cost-effective, but the optimized configuration achieves much higher hydrogen output and production reliability, which outweighs the modest increase in energy use.

4.3.2 CAPEX

The differences between the original and optimized scenarios are also reflected in the capital investment required for them. To get the values for the CAPEX, ROGER has provided their business case for their design. Values from the business case will be used to estimate the CAPEX of all the scenarios. The results from this are found in Table 4.4.

TABLE 4.4: Capital investment cost comparison of system components.

Component	Business case (€)	Original (€)	Optimized (€)
Underground storage	6,347,736	6,347,736	6,347,736
Filling compressors	690,000	828,000	993,600
Compressor to 500 bar	13,585,064	13,585,064	16,302,076.80
Filling stations	1,893,156	1,893,156	2,271,787.20
Total	22,515,956	22,653,956	25,915,200

As shown in the table, both scenarios use the same costs for the underground storage tanks, since this does not vary between scenarios. The costs for the filling stations are increased in the optimized design, as the number of filling stations is increased from five to six, and the costs are increased accordingly. In the business case, compression is assumed to occur from 40 to 70 bar, which requires only a single compressor stage. However, compressing from 40 to 100 bar needs two stages. The addition of a compressor stage increases costs due to the higher system complexity and the need for additional intercooling. Therefore, it is assumed that adding one compressor stage increases the total compressor cost by 20%. In the optimized scenario, three compressor stages are required, resulting in an additional 20% cost increase for both compressor systems, compared to the two-stage configuration. The increase in costs for the 500-bar compressor system by 20% significantly raises the total CAPEX of the optimized design.

4.3.3 OPEX and LCHS

The OPEX consist of two main factors: maintenance and energy costs. The maintenance costs are estimated as a percentage of the CAPEX. The exact percentage of the CAPEX per component was determined in Chapter 3.7. The total OPEX of the two designs are given in Table 4.5.

TABLE 4.5: Annual operational cost comparison for the original and optimized system designs.

Type of costs	Original design (€)	Optimized design (€)
Maintenance costs	728,533.28	855,196.73
Energy costs	411,443.59	640,150.11
Total	1,139,976.87	1,495,346.84

The OPEX of the two designs can then be used, in combination with the CAPEX, to determine the LCHS. This has been calculated using the Net Present Cost (NPC), using a project lifetime of 20 years and assuming a nominal discount rate of 6%. The NPC is then divided by the hydrogen output over the lifetime of the project to calculate the LCHS. The results of these calculations are given in Table 4.6.

TABLE 4.6: Economic performance comparison between the original and optimized system designs.

Parameter	Original design	Optimized design
Net Present Cost (€)	35,729,401	43,066,710
Total hydrogen output (1 year) (kg)	1,960,053	2,988,419
Total hydrogen output (20 years) (kg)	39,201,052	59,768,371
Levelized Cost of Hydrogen Storage (€/kg)	0.91	0.72

Table 4.6 shows that the Levelized Cost of Hydrogen Storage (LCHS) decreases significantly when moving from the original to the optimized design (from 0.91 to 0.72 €/kg). This reduction is primarily driven by the substantial increase in hydrogen output achieved by the optimized system. Although the optimized design has higher capital (CAPEX), operational (OPEX), and energy costs, the increased hydrogen output more than compensates for these higher expenses, resulting in a lower overall cost per kilogram of hydrogen delivered.

Overall, the economic evaluation shows that the optimized configuration represents a more cost-efficient and technically feasible design, despite its higher initial investment requirements.

Chapter 5

Conclusion

This study investigated the technical and economic performance of a proposed hydrogen storage system, which was designed to serve as a buffer between variable renewable hydrogen production and continuous hydrogen demand from transportation. Using a dynamic model developed in Python, different operational key parameters were evaluated to identify improvements to the current design. The current and possible new designs were evaluated, using technical and economic KPIs.

The result demonstrated that the current design proposed by ROGER Energy, operating five days per week with a pressure configuration of 100-70 bar, has reduced stability during fluctuations of the production rate. It also has trouble during the non-operational days, as it fills up frequently, leading to over saturation of the storage.

Multiple simulations were performed, where the pressure configuration, number of filling stations, and operational days were varied. Increasing the storage capacity (via pressure configuration), was found to be beneficial up to a certain point. Increasing the storage capacity further would only put more strain on the system, and not have more output. Increasing the number of filling stations and/or the operational days, both had a beneficial impact on the system in terms of output, but do require a larger storage capacity to be stable.

The system with the highest output was found to be a combination of increasing the number of filling stations and the number of operational days, both to six. To have stable fuelling operations, the pressure configuration was determined at 160-50. Therefore, the new optimized scenario was presented, which contains six filling stations and operates six days per week, at a pressure configuration of 160-50.

Implementing this optimized design, saw an increase of the realized production from 59.79% to 91.61%, and an increase in total hydrogen output by approximately 52%. Furthermore, the average delay per truck decreased from 10.06 to 3.37 minutes, providing more stability in the delivery of the hydrogen at the filling stations.

Increasing the pressure range from 100-70 to 160-50, did lead to a decrease in energy efficiency, as energy consumption per kg of output increased from 2.18 to 2.39 kWh per kg of hydrogen. However, a smaller difference in energy cost per kg was observed, as it increased from 0.210 to 0.214 €/kg. This is caused by a lower average energy price on Saturday, than on Monday to Friday.

Finally, the Levelized Cost of Hydrogen Storage (LCHS), decreased when going from the original to the optimized design, from 0.91 to 0.72 €/kg.

Overall, the optimized design significantly improves both the technical and economic performance of the hydrogen storage system. The reduction in leveled costs, increased output, and improved operational stability demonstrate the system's potential to enhance hydrogen supply reliability. The results of this study might help ROGER Energy in further optimizing its system design and may also contribute to the development of new hydrogen-related projects. In a broader context, these improvements could help accelerate hydrogen adoption in the Netherlands and support the ongoing transition toward a more sustainable energy system.

5.1 Recommendations

Based on the results of this study, it is recommended that ROGER Energy increases the number of filling stations and number of operational days from five to six. This adjustment increases both technical and economic performance significantly. For stable operations, a pressure configuration of 160-50 is required. However, if, due to technical or safety constraints, a maximum pressure of 160 bar cannot be achieved, it can be lowered. This will cause significantly more delay, but a less significant decrease in hydrogen output.

Furthermore, this study used literature-based assumptions for the maximum pressure. If specific design or safety constraints limit the achievable pressure range, additional research should be conducted to determine the optimal and safe maximum pressure for the system.

Further improvements to the current model can also be considered. For example, a tighter integration between hydrogen production and storage could allow the production rate to be adjusted dynamically based on the storage level. Additionally, incorporating demand forecasting would enable the system to anticipate future consumption and regulate hydrogen production more effectively.

Finally, the dynamic model applied simplified operational control logic compared to real-world operations. Future work should focus on developing and integrating a more detailed operational control strategy into the model to better represent actual system behaviour. Additionally, incorporating artificial intelligence or machine learning techniques could enable more adaptive and efficient operation, potentially leading to further performance improvements and new operational insights.

Bibliography

- [1] S. Shiva Kumar and V. Himabindu. Hydrogen production by pem water electrolysis – a review. *Materials Science for Energy Technologies*, 2(3):442–454, 2019.
- [2] Md Monjur Hossain Bhuiyan and Zahed Siddique. Hydrogen as an alternative fuel: A comprehensive review of challenges and opportunities in production, storage, and transportation. *International Journal of Hydrogen Energy*, 102:1026–1044, 2025.
- [3] Young C. Khan, M.A., C. MacKinnon, and D. Layzell. The techno-economics of hydrogen compression. *Transition Accelerator Technical Briefs*, 1, 2021.
- [4] Zainul Abdin, Kaveh Khalilpour, and Kylie Catchpole. Projecting the leveledized cost of large scale hydrogen storage for stationary applications. *Energy Conversion and Management*, 270:116241, 2022.
- [5] NASA. The effects of climate change. Available at: <https://science.nasa.gov/climate-change/effects/>.
- [6] Nature. What the war in ukraine means for energy, climate and food. Available at: <https://www.nature.com/articles/d41586-022-00969-9>.
- [7] European Commission. 2050 long-term strategy.
- [8] Netherlands Enterprise Agency. New offshore wind farms.
- [9] International Renewable Energy Agency. Decarbonising hard-to-abate sectors with renewables, perspectives for the g7. 2024.
- [10] Rijksoverheid. Sustainable energy, hydrogen.
- [11] HyungKuk Ju, Sukhvinder Badwal, and Sarbjit Giddey. A comprehensive review of carbon and hydrocarbon assisted water electrolysis for hydrogen production. *Applied Energy*, 231:502–533, 2018.
- [12] Pavlos Nikolaidis and Andreas Poullikkas. A comparative overview of hydrogen production processes. *Renewable and Sustainable Energy Reviews*, 67:597–611, 2017.
- [13] Meng Ni, Michael K.H. Leung, and Dennis Y.C. Leung. Technological development of hydrogen production by solid oxide electrolyzer cell (soec). *International Journal of Hydrogen Energy*, 33(9):2337–2354, 2008.
- [14] Kalpana Chaudhary, Kartikey Bhardvaj, and Ayushi Chaudhary. A qualitative assessment of hydrogen generation techniques for fuel cell applications. *Fuel*, 358:130090, 2024.

- [15] Muhammad R. Usman. Hydrogen storage methods: Review and current status. *Renewable and Sustainable Energy Reviews*, 167:112743, 2022.
- [16] P. Muthukumar, Alok Kumar, Mahvash Afzal, Satyasekhar Bhogilla, Pratibha Sharma, Abhishek Parida, Sayantan Jana, E Anil Kumar, Ranjith Krishna Pai, and I.P. Jain. Review on large-scale hydrogen storage systems for better sustainability. *International Journal of Hydrogen Energy*, 48(85):33223–33259, 2023.
- [17] H. Barthelemy, M. Weber, and F. Barbier. Hydrogen storage: Recent improvements and industrial perspectives. *International Journal of Hydrogen Energy*, 42(11):7254–7262, 2017. Special issue on The 6th International Conference on Hydrogen Safety (ICHS 2015), 19-21 October 2015, Yokohama, Japan.
- [18] Qusay Hassan, Sameer Algburi, Aws Zuhair Sameen, Marek Jaszcuzur, and Hayder M Salman. Hydrogen as an energy carrier: properties, storage methods, challenges, and future implications. *Environment Systems and Decisions*, 44(2):327–350, 2024.
- [19] Ramin Moradi and Katrina M. Groth. Hydrogen storage and delivery: Review of the state of the art technologies and risk and reliability analysis. *International Journal of Hydrogen Energy*, 44(23):12254–12269, 2019.
- [20] G. AlZohbi, A. Almoaikel, and L. AlShuhail. An overview on the technologies used to store hydrogen. *Energy Reports*, 9:28–34, 2023. Proceedings of 2022 7th International Conference on Renewable Energy and Conservation.
- [21] Alexis Munyentwali, Khai Chen Tan, and Teng He. Advancements in the development of liquid organic hydrogen carrier systems and their applications in the hydrogen economy. *Progress in Natural Science: Materials International*, 34(5):825–839, 2024.
- [22] Nidhi Garg, Ankita Sarkar, and Basker Sundararaju. Recent developments on methanol as liquid organic hydrogen carrier in transfer hydrogenation reactions. *Coordination Chemistry Reviews*, 433:213728, 2021.
- [23] G. Sdanghi, G. Maranzana, A. Celzard, and V. Fierro. Review of the current technologies and performances of hydrogen compression for stationary and automotive applications. *Renewable and Sustainable Energy Reviews*, 102:150–170, 2019.
- [24] Ahmed M. Elberry, Jagruti Thakur, Annukka Santasalo-Aarnio, and Martti Larmi. Large-scale compressed hydrogen storage as part of renewable electricity storage systems. *International Journal of Hydrogen Energy*, 46(29):15671–15690, 2021.
- [25] Ujwal Shreenag Meda, Nidhi Bhat, Aditi Pandey, K.N. Subramanya, and M.A. Lourdu Antony Raj. Challenges associated with hydrogen storage systems due to the hydrogen embrittlement of high strength steels. *International Journal of Hydrogen Energy*, 48(47):17894–17913, 2023.
- [26] Lei Zhang, Cunqi Jia, Fuqiao Bai, Wensen Wang, Senyou An, Kaiyin Zhao, Zihao Li, Jingjing Li, and Hai Sun. A comprehensive review of the promising clean energy carrier: Hydrogen production, transportation, storage, and utilization (hptsu) technologies. *Fuel*, 355:129455, 2024.
- [27] Kashif Naseem, Fei Qin, Faryal Khalid, Guoquan Suo, Taghazal Zahra, Zhanjun Chen, and Zeshan Javed. Essential parts of hydrogen economy: Hydrogen production, storage, transportation and application. *Renewable and Sustainable Energy Reviews*, 210:115196, 2025.

- [28] The description and properties of the Multibrid M5000. Available at: <https://en.wind-turbine-models.com/turbines/22-multibrid-m5000>.
- [29] CoolProp is a thermo-physical property library which gives accurate real gas thermodynamic values. It is also open source. Available at: <https://coolprop.org/>.
- [30] SAE International. Fueling protocols for light duty gaseous hydrogen surface vehicles, 2020. SAE International Standard, Published May 2020.
- [31] Fu Wing Yu, K.T. Chan, R.K.Y. Sit, and J. Yang. Review of standards for energy performance of chiller systems serving commercial buildings. *Energy Procedia*, 61:2778–2782, 12 2014.
- [32] U.S. Department of Energy. Hydrogen delivery infrastructure options analysis. Technical report, Office of Hydrogen, Fuel Cells & Infrastructure Technologies Program, 2005. Accessed: 2025-11-17.
- [33] National Renewable Energy Laboratory (NREL). Hydrogen station compression, storage, and dispensing technical status and costs. Technical Report NREL/TP-5400-58564, National Renewable Energy Laboratory (NREL), Golden, CO, USA, 2014. DOE Hydrogen and Fuel Cells Program Record, accessed October 2025.
- [34] Andreas Zauner Charlotte van Leeuwen. D8.3 – final report on the economic assessment of power-to-gas concepts. Technical report, STORE&GO Project, 2018.

Appendix A

Model Assumptions

For the model and its calculations, certain assumptions have been made. The total list of these assumptions is given below.

System Design and Operational Assumptions

- The number of tanks that can empty at the same time is five, set equal to the original number of filling stations. The same goes for the number of tanks that can be filled at the same time.
- The volume of the piping system is not taken into account in the model.
- It is assumed that there is no time delay between the different components in the model. As the simulation is iteratively per minute, it is assumed that within this time period, the hydrogen can flow to the right part of the system. The additional time it would take for hydrogen to travel through a piping system is negligible compared to the total simulation time.
- The balancing step, done when none of the tanks in *Emptying* state are switched to either *Idle* or *Filling state*, will require a mass difference. This difference is assumed to be 10%.
- The capacity of a container is assumed to be 280 kg at 500 bar.

Thermodynamic Assumptions

- It is assumed there is no temperature loss to the environment from the tanks. The tanks are placed underground, which should keep heat transfer to the environment to a minimum.
- The assumption is made that there is no pressure loss in the system.
- The isentropic efficiency is assumed to be 65%, based on [3].
- The COP is assumed to be 3, based on [31].
- The mechanical efficiency of the compressor is assumed to be 90%.
- The maximum temperature that can be reached during compression is 85°C, based on [30].

Economic Assumptions

- The discount rate is assumed to be 6%, based on the business case of ROGER.
- When adding a compressor stage, it is assumed that the total cost of the compressor is increased by 20%, based on [32].
- An increase in the number of filling stations is assumed to be accompanied by a linear increase in costs.

Appendix B

Thermodynamic calculations

The total energy consumption is calculated using CoolProp, which gives real gas values for the enthalpy and entropy, based on the pressure and temperature. Coolprop is also used in determining the number of stages for each compressor, by calculating the outlet temperature after each compressor stage. Determining the energy consumption of a compressor follows this calculation pattern:

For N stages, the compression ratio is:

$$\text{CR}_{\text{stage}} = \left(\frac{p_{\text{out}}}{p_{\text{in}}} \right)^{1/N} \quad (\text{B.1})$$

Where CR_{stage} is the compression ratio, p_{in} is the inlet pressure, and p_{out} is the outlet pressure. The outlet pressure is then:

$$p_{2,i} = p_{1,i} \cdot \text{CR}_{\text{stage}}, \quad (\text{B.2})$$

where $p_{1,i}$ and $p_{2,i}$ denote the inlet and outlet pressures of stage i .

For each stage i , the inlet enthalpy and entropy are obtained with CoolProp at their current pressure and temperature:

$$h_{1,i} = h(p_{1,i}, T_{\text{in}}), \quad s_{1,i} = s(p_{1,i}, T_{\text{in}}). \quad (\text{B.3})$$

From this, the isentropic outlet enthalpy is determined by keeping the entropy constant:

$$h_{2s,i} = h(p_{2,i}, s_{1,i}). \quad (\text{B.4})$$

Then calculating the real outlet enthalpy by using the isentropic efficiency:

$$\eta_c = \frac{h_{2s,i} - h_{1,i}}{h_{2a,i} - h_{1,i}} \implies h_{2a,i} = h_{1,i} + \frac{h_{2s,i} - h_{1,i}}{\eta_c} \quad (\text{B.5})$$

The specific work of stage i is then:

$$w_{\text{comp},i} = h_{2a,i} - h_{1,i}. \quad (\text{B.6})$$

After the compression stage, the hydrogen must be cooled back to the inlet temperature (10°C). The heat that needs to be removed to achieve this, is equal to the difference between the outlet enthalpy, and the enthalpy at the same pressure but at 10°C . The enthalpy after cooling is:

$$h_{\text{cool},i} = h(p_{2,i}, T_{\text{in}}). \quad (\text{B.7})$$

The heat that must be removed is thus:

$$q_{\text{cool},i} = h_{2a,i} - h_{\text{cool},i}. \quad (\text{B.8})$$

With the required heat removal known, the work needed for the cooling can be calculated by using the COP:

$$w_{\text{cool},i} = \frac{q_{\text{cool},i}}{\text{COP}}. \quad (\text{B.9})$$

Now, the total energy requirement can be calculated, which consists of the compressor work and the cooling work. The total compressor work is corrected by the mechanical efficiency:

$$w_{\text{comp,tot}} = \frac{\sum_{i=1}^N w_{\text{comp},i}}{\eta_{\text{mech}}}. \quad (\text{B.10})$$

The total cooling work is:

$$w_{\text{cool,tot}} = \sum_{i=1}^N w_{\text{cool},i}. \quad (\text{B.11})$$

Thus, the total specific energy consumption is:

$$w_{\text{tot,spec}} = w_{\text{comp,tot}} + w_{\text{cool,tot}}. \quad (\text{B.12})$$

Multiplying the specific energy requirement by the hydrogen mass flow rate \dot{m}_{H_2} (kg/min) yields the energy consumption per time step:

$$\dot{E}_{\text{fill}} = w_{\text{tot,spec}} \cdot \dot{m}_{\text{H}_2}, \quad (\text{B.13})$$